A Generic Simulation Approach for the Fast and Accurate Estimation of the Outage Probability of Single Hop and Multihop FSO Links Subject to Generalized Pointing Errors

This article has been accepted for publication in a future issue of this journal, but has not been fully edited. Content may change prior to final publication. Citation information: DOI 10.1109/TWC.2017.2731947, IEEE Transactions on Wireless Communications

A Generic Simulation Approach for the Fast and Accurate Estimation of the Outage Probability of Single Hop and Multihop FSO Links Subject to Generalized Pointing Errors

Chaouki Ben Issaid, Ki-Hong Park, and Mohamed-Slim Alouini

***Abstract*—When assessing the performance of the free space optical (FSO) communication systems, the outage probability encountered is generally very small, and thereby the use of nave Monte Carlo simulations becomes prohibitively expensive. To estimate these rare event probabilities, we propose in this work an importance sampling approach which is based on the exponential twisting technique to offer fast and accurate results. In fact, we consider a variety of turbulence regimes, and we investigate the outage probability of FSO communication systems, under a generalized pointing error model based on the Beckmann distribution, for both single and multihop scenarios. Selected numerical simulations are presented to show the accuracy and the efficiency of our approach compared to naive Monte Carlo.**

***Index Terms*—Free-space optical communication, pointing errors, atmospheric turbulence, importance sampling, exponential twisting, multihop.**

I. Introduction

FREE-space optical (FSO) communication presents an interesting alternative to radio wave and optical cables to meet the growing needs of telecommunication regarding high data rates. However, the design of the FSO links needs to take into consideration two main challenges: (i) the atmospheric turbulences and (ii) the pointing errors. These factors cause random fluctuations of the received signal and thereby disrupt the performance of the link.

Pointing errors have two major components: (i) a deterministic error related to the boresight which is a fixed displacement between the detector and beam centers and (ii) a random error jitter which represents the offset from the beam center at the detector plane. Many works investigated the effect of the pointing errors on the performance of FSO systems. In [2], Arnon determined the optimal divergence angle as a function of the bit error probability taking into consideration the jitter caused by the building sway. A novel statistical model for pointing errors was presented in [3] by Farid and Hranilovic taking into account the jitter variance, the beam width, and the detector size. The authors derived expressions for the outage probability for both weak and strong turbulence regimes assuming zero boresights. In [4], Gappmair *et al.* generalized the Rayleigh model for misalignments by using the Hoyt distribution. In their letter, an approximate expression for the average bit error rate (BER) of an FSO link under Gamma-Gamma turbulence is obtained. Later on, a more general model assuming non-zero boresights but same jitter effects was proposed and studied by Yang *et al.* in [5]. The authors studied the BER as well as the outage probability for FSO system under different atmospheric conditions. In [6], Al-Quwaiee *et al.* derived an asymptotic expression for the ergodic capacity under a generalized pointing error model when the radial displacement follows a Beckmann distribution allowing both boresight and different jitter intensities in horizontal and vertical directions. Since the ergodic capacity is not always the most suitable performance metrics for FSO systems, we consider, in this paper, a general pointing error model, similar to the one studied in [6], and propose a fast simulation approach to accurately estimate the outage probability (or equivalently the outage capacity) of FSO systems under these conditions.

Atmospheric turbulence happens as a result of the random changes in the refractive index of the air. This leads to changes in the path that the light takes in its propagation through the air, and thus causes fluctuations of the received signal. Some papers, including [2], [7] as examples, investigated the consequences of atmospheric turbulence on the error rates of FSO links. Scintillations have been described using various statistical models [8]-[9]. In weak turbulence regime, the most appropriate model is the lognormal, while the Gamma-Gamma is widely used to model signal fluctuations in the strong turbulence regime. Recently, the performance of FSO links under new turbulence models has been studied. In [10], the authors derived approximate and closed-form expressions for the ergodic capacities of FSO systems under nonzero boresight errors where the radial displacement r is assumed to follow a Rician distribution. The atmospheric turbulence is modeled using three probability density functions (PDFs): the lognormal, the Rician-lognormal and the Málaga distribution. The analysis is carried out for both intensity modulation/direct detection (IM/DD) and heterodyne detection. More attention has been paid to the Málaga turbulence channel in [11] where unified expressions for the PDF, the cumulative density function (CDF), the moment generating function (MGF), and the moments of the average SNR of an FSO link were presented. Using these results, closed-form and asymptotic

The authors are in the Computer, Electrical and Mathematical Science and Engineering (CEMSE) Division, King Abdullah University of Science and Technology (KAUST), Thuwal, Makkah Province, Saudi Arabia (e-mail: {chaouki.benissaid, kihong.park, slim.alouini}@kaust.edu.sa).

This work is supported by the KAUST-KFUPM research initiative.

Part of this work was presented at the IEEE Global Communications Conference (GLOBECOM'2016), Washington, DC , USA, Dec. 2016 [1].

This article has been accepted for publication in a future issue of this journal, but has not been fully edited. Content may change prior to final publication. Citation information: DOI 10.1109/TWC.2017.2731947, IEEE Transactions on Wireless Communications

expressions are derived for performance metrics, such as the outage probability, the average BER and the ergodic capacity. The analysis is done assuming zero boresight errors and under the IM/DD and heterodyne detection.

An efficient technique to enhance the reliability of FSO links is to resort to multihop relaying where the signal is transmitted from the source to the destination by means of intermediate terminals. In [12], Kazemlou *et al.* investigated the BER performance of an all-optical FSO system for both amplify-and-forward (AF) and decode-and-forward (DF) using Monte Carlo simulations. The system performance was studied under weak turbulence regime and the authors assumed either fixed-gain optical amplifiers or optical regenerators. They showed that the total communicating distance of a two-hops system has increased by 0.9 km for the AF case and by 1.9 km in the regenerate-and-forward scenario compared to the direct transmission at a BER of 10^{-5}. Both serial and parallel relay-assisted transmission FSO communication systems have been investigated in [13]. The authors derived the outage probability of both systems for DF and AF modes in the presence of lognormal turbulence. They showed that adding a single relay at an outage probability of 10^{-6} results in a performance improvement of 18.5 dB. In [14], the authors presented novel experimental results for an all-optical AF relay-assisted 10 Gbps FSO link over Gamma-Gamma turbulence channel. Mohd Nor *et al.* derived expressions for the end-to-end SNR as well as the BER and showed that a good agreement between the experimental results and the mathematical derivations exists especially at high SNR. In [15], the authors studied the performance of dual-hop RF/FSO system in the presence of pointing errors. In this work, the FSO link is assumed to operate over Gamma-Gamma fading and Rayleigh model for misalignments is considered. The performance of multihop FSO links operating over Gamma-Gamma turbulence in the presence of pointing errors and path-loss effects is investigated in [16]. The mutihop system in this case uses channel-state-information-assisted and fixed-gain relays. Tang *et al.* derived closed-form expressions for the MGF, PDF, as well as the CDF of this system. In [17], Zedini *et al.* studied the end-to-end performance of multihop FSO system operating over Gamma-Gamma turbulence fading in the presence of pointing error impairments. Two types of relays were considered: (i) amplify-and-forward channel state-information-assisted, or (ii) fixed-gain relays. The authors provided closed-form bounds for the outage probability, the average BER, as well as the ergodic capacity of on-off keying modulation scheme.

Finding a closed-form expression for the outage probability is not always feasible. To the best of our knowledge, no closed-form results for the outage probability of FSO links over generalized pointing errors were derived in the literature. In this case, one can use a numerical approximation based for instance on the Monte Carlo (MC) method. However, since FSO systems are often used for high-speed backhaul links, the outage probability requirements are typically very low, i.e. of the order of 10^{-8}, thereby a very large number of samples is required to guarantee a good quality estimator. An alternative method to reduce the number of samples is the importance sample (IS) technique [18]. The interest of this method lies in the possibility of exhibiting a change of law, i.e. instead of using samples from a PDF $f(\cdot)$, samples from a new PDF $f^*(\cdot)$ are used to guarantee that a certain event takes place more frequently, which reduces the variance of the standard MC estimator. While IS method has been widely used for the performance evaluation of digital communication systems, in particular to study the performance of avalanche photodiodes [19], fiber repeaters [20], and generic digital communication systems [21], they have not been applied for the evaluation of the performance of FSO systems. A concise review of the use of IS in communication systems can be found in [22].

In [1], we used an efficient IS approach based on the exponential twisting technique to study the outage probability of FSO system under a generalized pointing error model with different vertical and horizontal jitter effects and a nonzero boresight for the specified lognormal and Gamma-Gamma models. In this paper, we extend the work to more general types of turbulence, more specifically Rician-lognormal, Málaga, and Double Generalized Gamma models while including detailed proofs of the derivations. We also show how our approach can be extended to estimate bounds on the outage probability for the multihop systems. The reminder of this paper is organized as follows. We start by describing the structure of the FSO system in Section II, as well as the pointing errors and the atmospheric turbulence statistical models. We then provide in Section III a brief description of the fundamental concepts of IS method as well as the tools required to estimate the outage probability in our particular set-up. Then, we briefly explain in section IV how to generalize our proposed approach to estimate bounds on the outage probability in the multihop case. In Section V, we show some selected numerical results related to the outage probability under different turbulence regimes. In this section, we first establish the efficiency of the IS method compared to MC method. In fact, we show that IS provides a significant reduction in the number of samples, especially for low outage probability values. We then study, using IS, the impact of the difference in the horizontal and vertical jitter effects on the outage probability, as well as the effect of the severity and type of turbulence for the same pointing error conditions. Before concluding, we provide numerical simulations for the estimation of the outage probability bounds for the multihop case.

II. System Model

In this work, we study the performance of standard FSO systems with IM/DD in which the received signal y can be modeled as

$$y = hx + n, \tag{1}$$

where h is the channel fading, x is the transmitted signal, and n is a zero mean Gaussian noise with variance σ_n^2. The signal x is assumed to have an average transmitted optical power P_t. Let h_l denote the path loss, h_p the pointing error loss factor, and h_a the atmospheric turbulence loss factor. We consider a composite fading channel, where $h = h_l h_a h_p$. Here, unlike the random variables (RVs) h_p and h_a, h_l is considered to be a constant. Following [3], [5], we assume that h_p and h_a are

This article has been accepted for publication in a future issue of this journal, but has not been fully edited. Content may change prior to final publication. Citation information: DOI 10.1109/TWC.2017.2731947, IEEE Transactions on Wireless Communications

independent RVs. In this setting, the received signal-to-noise ratio (SNR) is defined as

$$\gamma = \gamma_0 h^2, \tag{2}$$

where $\gamma_0 \triangleq \frac{2P_t^2}{\sigma_n^2}$ and the outage probability is defined as

$$P_{\text{out}}(\gamma_{th}) = \mathbb{P}(\gamma < \gamma_{th}) = \mathbb{P}(h < h_{th}), \tag{3}$$

where γ_{th} is a given threshold and $h_{th} \triangleq \sqrt{\frac{\gamma_{th}}{\gamma_0}}$.

Although the work presented in this paper deals with the outage probability, our approach is easily applicable for the evaluation of the outage capacity[1]. In fact, given the very high data rates achieved by FSO over atmospheric turbulent channels, these channels are typically viewed as slowly varying channels and with a coherence time greater than the latency requirement. Hence, in this case, ergodic/average capacity is not always considered as the most suitable performance metric. Rather outage capacity is considered to be a more realistic metric of channel capacity for FSO systems [3] [26, Chap. 4].

A. Pointing Errors

Let z denote the distance between the transmitter and the detector, and r the radial displacement between the detector center, assumed to be circular with aperture radius a and a Gaussian beam center. The beam spot at the detector plane is considered to be symmetrical with respect to its origin and the turbulence is assumed to be isotropic. In this work, the pointing errors represent the misalignment between the transmitter and the receiver which results from the displacement of the laser beam in either the horizontal or the vertical direction, i.e. we are considering a $2D$ configuration. We assume that the transmitter and the receiver plans are parallel and that the laser beam is perpendicular to the receiver area. Under these assumptions, the expression of the pointing error loss factor is approximated by [3] as

$$h_p(r,z) \approx A_0 \exp\left(-\frac{2r^2}{w_{zeq}^2}\right), \tag{4}$$

where w_{zeq} is the equivalent beam width and A_0 is the fraction of the collected power at $r = 0$. In [3], the authors show that (4) is a good approximation as long as $\frac{w_z}{a} > 6$, where w_z is the beamwidth.

Let r_x and r_y denote, respectively, the horizontal and vertical displacement of the beam in the detector plane. If $r_x \sim \mathcal{N}(\mu_x, \sigma_x^2)$ and $r_y \sim \mathcal{N}(\mu_y, \sigma_y^2)$ are independent then the radial displacement $r = \sqrt{r_x^2 + r_y^2}$ follows the Beckmann distribution [27]

$$f_r(r) = \frac{r}{2\pi\sigma_x\sigma_y} \times \int_0^{2\pi} \exp\left(-\frac{(r\cos\phi - \mu_x)^2}{2\sigma_x^2} - \frac{(r\sin\phi - \mu_y)^2}{2\sigma_y^2}\right) d\phi \; U(r), \tag{5}$$

where $U(\cdot)$ is the unit step function.

The Beckmann distribution is a PDF that generalizes other PDFs, e.g. Rayleigh when $\mu_x = \mu_y = 0$, $\sigma_x = \sigma_y$, Hoyt (Nakagami-q) when $\mu_x = \mu_y = 0$, $\sigma_x \neq \sigma_y$, and Rician (Nakagami-n) when $\sqrt{\mu_x^2 + \mu_y^2} \neq 0$, $\sigma_x = \sigma_y$.

B. Atmospheric Turbulence

1) Lognormal Turbulence: For weak turbulence regime, we consider the lognormal model to describe the atmospheric fading. The PDF of h_a is thus given by

$$f_{h_a}(h_a) = \frac{1}{h_a\sqrt{2\pi\sigma_R^2}} \exp\left(-\frac{(\log(h_a) + \frac{\sigma_R^2}{2})^2}{2\sigma_R^2}\right) \; U(h_a), \tag{6}$$

where σ_R^2 is the Rytov variance for a plane wave. The distinction between the two turbulence regimes is made based on the magnitude of the Rytov variance. According to [28], a Rytov variance less than 0.3 corresponds to a weak turbulence, while moderate to strong turbulence is characterized by a value greater than 0.3.

2) Rician-Lognormal Turbulence: In general, atmospheric turbulence can be modeled as the product of two independent RVs: (i) a Rice RV that represents the small-scale turbulence and (ii) a lognormal RV for the large-scale turbulence. In this case, the PDF of the atmospheric turbulence is given by [9, Eq. (5)]

$$f_{h_a}(h_a) = \frac{(1+k^2)\exp(-k^2)}{\Omega\sqrt{2\pi}\sigma_R} \times \int_0^\infty \exp\left(-\frac{(1+k^2)h_a}{z\Omega} - \frac{(\log(z) + \frac{\sigma_R^2}{2})^2}{2\sigma_R^2}\right) \times \mathrm{I}_0\left(2k\sqrt{\frac{1+k^2}{z\Omega}h_a}\right)\frac{dz}{z^2}, \tag{7}$$

where Ω is the average fading power, $k > 0$ is the Rician turbulence parameter, and $\mathrm{I}_0(\cdot)$ is the zeroth-order modified Bessel function of the first kind [29, Sec. 8.431].

3) Málaga Turbulence: A more general turbulence model is known as the Málaga turbulence [30]. In this case, the atmospheric fading can be seen as the product of two RVs: (i) $Y \triangleq |R|^2$ for small-scale turbulence and (ii) X for large-scale turbulence, where

$$R = \sqrt{G}\left(\sqrt{\Omega}\ \exp(j\phi_A) + \sqrt{2b_0\rho}\ \exp(j\phi_B)\right) + \sqrt{1-\rho}\, U. \tag{8}$$

The large-scale fluctuations, X, follows a Gamma PDF

$$f_X(x) = \frac{\alpha^\alpha}{\Gamma(\alpha)} x^{\alpha-1}\exp(-\alpha x), \tag{9}$$

while G has a Gamma distribution such that $\mathbb{E}[G] = 1$ and $\text{Var}[G] = \frac{1}{\beta}$ and U is circular Gaussian complex RV. Here, Ω denote the average power of the line-of-sight (LOS) component, $2b_0$ represents the average power of the total scatter and $\rho \in [0,1]$ measures the fraction of the scattering power to the LOS component. The PDF of Málaga turbulence is given by [30, Eq. (24)]

$$f_{h_a}(h_a) = A\sum_{m=1}^{\beta} a_m h_a^{\frac{\alpha+m}{2}-1} K_{\alpha-m}\left(2\sqrt{\frac{\alpha\beta h_a}{g\beta + \Omega_0}}\right) \tag{10}$$

[1]The outage capacity is defined as the transmission rate R_0 which satisfies $\mathbb{P}(C(\gamma) < R_0) = \mathbb{P}(\gamma < \gamma_{th} = C^{-1}(R_0)) = P_{\text{out}}(C^{-1}(R_0)) = p_0$ where p_0 is a given value and $C(\cdot)$ is the instantaneous capacity. In FSO, a tight lower bound of $C(\gamma)$ is given by $\log_2(1 + d\gamma)$ where $d = 1$ for heterodyne detection and $d = \frac{e}{2\pi}$ for IM/DD [11] [23] [24, Eq. (7.43)] [25, Eq. (26)]. Thus $\gamma_{th} = C^{-1}(R_0) = \frac{2^{R_0}-1}{d}$.

This article has been accepted for publication in a future issue of this journal, but has not been fully edited. Content may change prior to final publication. Citation information: DOI 10.1109/TWC.2017.2731947, IEEE Transactions on Wireless Communications

where $g = 2b_0(1-\rho)$, and

$$\begin{aligned} A &\triangleq \frac{2\alpha^{\frac{\alpha}{2}}}{g^{1+\frac{\alpha}{2}}\Gamma(\alpha)}\left(\frac{g\beta}{g\beta+\Omega_0}\right)^{\frac{\alpha}{2}+\beta}, \\ a_m &\triangleq \binom{\beta-1}{m-1}\frac{(g\beta+\Omega_0)^{1-\frac{m}{2}}}{(m-1)!}\left(\frac{\Omega_0}{g}\right)^{m-1}\left(\frac{\alpha}{\beta}\right)^{\frac{m}{2}}, \\ \Omega_0 &= \Omega + 2b_0\rho + 2\sqrt{2b_0\rho\Omega}\,\cos(\phi_A-\phi_B). \end{aligned} \quad (11)$$

The Málaga distribution is a PDF that generalizes other PDFs, lognormal when $\rho = 0$, and $g \to 0$, K-distribution when $\beta = 1$ or ($\rho = 0$ and $\Omega = 0$), and Gamma-Gamma distribution when $\rho \to 1$ and $\Omega_0 = 1$.

4) Double Generalized Gamma Turbulence: Under the assumption that both large and small scale turbulences follow a Generalized Gamma distribution [31, Eq. (1)], each with its specific shaping parameters, the product h_a follows a Double Generalized Gamma distribution whose PDF is given by [32]

$$f_{h_a}(h_a) = \frac{\alpha_2\lambda\sigma^{\beta_1-\frac{1}{2}}\lambda^{\beta_2-\frac{1}{2}}(2\pi)^{1-\frac{\sigma+\lambda}{2}}}{\Gamma(\beta_1)\Gamma(\beta_2)h_a} G^{0,\lambda+\sigma}_{\lambda+\sigma,0}\left[\left(\frac{\Omega_2}{h_a^{\alpha_2}}\right)^{\lambda}\frac{\lambda^{\lambda}\sigma^{\sigma}\Omega_1^{\sigma}}{\beta_1^{\sigma}\beta_2^{\lambda}}\,\middle|\,\begin{matrix}1-\kappa_0\\ -\end{matrix}\right], \quad (12)$$

where λ and σ are two positive integers such that $\frac{\lambda}{\sigma} = \frac{\alpha_1}{\alpha_2}$. For instance, given a certain value of λ, $\sigma = \lceil\frac{\lambda\alpha_2}{\alpha_1}\rceil$. Here, $\kappa_0 = \Delta(\sigma : \beta_1), \Delta(\lambda : \beta_2)$ where $\Delta(x : y) = \frac{y}{x}, \frac{y+1}{x}, \ldots, \frac{y+x-1}{x}$ and $G^{m,n}_{p,q}[\cdot]$ is the Meijers G-function defined in [29, Eq.(9.301)].

For a certain set of shaping parameters, the Double Generalized Gamma PDF can specify to other PDFs. When $\beta_i = 1$, it reduces to the Double-Weibull PDF. For $\alpha_i = 1$ and $\Omega_i = 1$, it coincides with the Gamma-Gamma distribution. When $\alpha_i \to 0$ and $\beta_i \to +\infty$, the Double Generalized Gamma distribution approximates very well the lognormal PDF, while if $\alpha_i = 1$, $\Omega_i = 1$, and $\beta_2 = 1$, it becomes the K-distribution.

III. Importance Sampling

In this section, we explain briefly the idea behind IS, and how to apply it for our purpose of estimating the outage probability. IS is a well-known method to evaluate the probability of rare events [18]. In fact, the advantage of this method lies in its simplicity and ease of implementation. It aims to reduce the variance of the MC estimator by introducing an auxiliary PDF. For a thorough explanation of the approach, the reader is directed to [18].

A. Key Idea

The interest of this work is to estimate the outage probability, (3), using fast simulation based on IS. First, we re-write the outage probability expression as

$$P_{\text{out}}(\gamma_{th}) = \mathbb{P}(h < h_{th}) = \mathbb{P}(y_a + y_p < \varepsilon), \quad (13)$$

where y_a and y_p denote respectively the logarithm of h_a and h_p, and $\varepsilon \triangleq \log\left(\frac{h_{th}}{h_l}\right)$.

First, we recall the standard MC estimator for P_{out} as

$$\text{I} = \frac{1}{N}\sum_{n=1}^{N}\mathbb{1}_{(y_{a,n}+y_{a,n}<\varepsilon)}, \quad (14)$$

where N is the sample size for the MC estimator and $y_{a,n}$ and $y_{p,n}$ are sampled from the original PDFs $f_{y_a}(\cdot)$ and $f_{y_p}(\cdot)$, respectively. The MC estimator (14) is an unbiased and consistent estimator of P_{out}.

Table I summarizes the PDF of y_a for the different atmospheric turbulence models.

The PDF of the pointing error, $f_{y_p}(\cdot)$, is given by (15) where $\xi_x = \frac{w_{zeq}}{2\sigma_x}$ and $\xi_y = \frac{w_{zeq}}{2\sigma_y}$.

The IS idea is based on the fact that the representation of P_{out} as an expected value is not unique. In fact, we can write

$$\begin{aligned} P_{\text{out}} &= \int\int \mathbb{1}_{(y_a+y_p<\varepsilon)} f_{y_a}(y_a) f_{y_p}(y_p) dy_a dy_p \\ &= \int\int \mathbb{1}_{(y_a+y_p<\varepsilon)} \omega_{y_a}(y_a)\omega_{y_p}(y_p) f^*_{y_a}(y_a) f^*_{y_p}(y_p) dy_a dy_p \\ &= \mathbb{E}^*[\mathbb{1}_{(y_a+y_p<\varepsilon)}\omega_{y_a}(y_a)\omega_{y_p}(y_p)], \end{aligned} \quad (16)$$

where $\mathbb{E}^*$ denotes the expected value with respect to (w.r.t) the biased PDFs $f^*_{y_a}(\cdot)$ and $f^*_{y_p}(\cdot)$ and the likelihood/weighting functions $\omega_{y_a}(\cdot)$ and $\omega_{y_p}(\cdot)$ are given by

$$\omega_{y_k}(\cdot) = \frac{f_{y_k}(\cdot)}{f^*_{y_k}(\cdot)},\ k \in \{a, p\}. \quad (17)$$

As such, the outage probability estimator using IS is given by

$$\text{I}^* = \frac{1}{N^*}\sum_{n=1}^{N^*}\mathbb{1}_{(y^*_{a,n}+y^*_{p,n}<\varepsilon)}\omega_{y_a}(y^*_{a,n})\omega_{y_p}(y^*_{p,n}), \quad (18)$$

where N^* is the sample size for the IS estimator, $y^*_{a,n}$ and $y^*_{p,n}$ are here sampled from the biased PDFs $f^*_{y_a}(\cdot)$ and $f^*_{y_p}(\cdot)$, respectively. The IS estimator is also an unbiased and consistent estimator of P_{out}. Note that we use * to denote the parameters and the densities that arise from the use of IS, to make the distinction with standard MC.

For comparison sake, we assume that the number of samples used to evaluate the IS and MC estimators is the same, N. The variance of the MC estimator is [18]

$$\text{Var}[I] = \frac{1}{N}(P_{\text{out}} - P^2_{\text{out}}), \quad (19)$$

while the variance of IS is given by [18]

$$\text{Var}^*[I^*] = \frac{1}{N}(\mathbb{E}^*[\mathbb{1}^2_{(y_a+y_p<\varepsilon)}\omega^2_{y_a}(y_a)\omega^2_{y_p}(y_p)] - P^2_{\text{out}}). \quad (20)$$

The IS method aims to find a proper biased PDFs $f^*_{y_a}(\cdot)$ and $f^*_{y_p}(\cdot)$ in order to minimize $\mathbb{E}^*[\mathbb{1}^2_{(y_a+y_p<\varepsilon)}\omega^2_{y_a}(y_a)\omega^2_{y_p}(y_p)]$. In the literature, different kind of techniques exist to accomplish this purpose. In this work, we use, as explained in Section III-B, the exponential twisting technique to fulfill this objective.

To show the efficiency of IS compared to MC, we introduce two notions: (i) the relative error and (ii) the gain indicator. The relative error of both methods, MC and IS, are defined as [33]

$$\begin{aligned} \epsilon_{MC} &= \frac{\alpha}{P_{\text{out}}}\sqrt{\frac{P_{\text{out}}(1-P_{\text{out}})}{N}}, \\ \epsilon_{IS} &= \frac{\alpha}{P_{\text{out}}}\sqrt{\frac{\text{Var}^*[\mathbb{1}_{(y_a+y_p<\varepsilon)}\omega_{y_a}(y_a)\omega_{y_p}(y_p)]}{N^*}}, \end{aligned} \quad (21)$$

This article has been accepted for publication in a future issue of this journal, but has not been fully edited. Content may change prior to final publication. Citation information: DOI 10.1109/TWC.2017.2731947, IEEE Transactions on Wireless Communications

TABLE I: PDF of y_a for different turbulence regimes.

Turbulence model	PDF of y_a : $f_{y_a}(x)$
Lognormal	$\frac{1}{\sqrt{2\pi}\sigma_R}\exp\left(-\frac{1}{2\sigma_R^2}\left(x+\frac{\sigma_R^2}{2}\right)^2\right)$
Rician-Lognormal	$\frac{(1+k^2)\exp(x)}{\Omega\sqrt{2\pi}\sigma_R}\int_0^{+\infty}\exp\left(-k^2-\frac{1+k^2}{z\Omega}\exp(x)\right)\mathrm{I}_0\left(2k\sqrt{\frac{1+k^2}{z\Omega}\exp(x)}\right)\exp\left(-\frac{1}{2\sigma_R^2}\left(\log(z)+\frac{\sigma_R^2}{2}\right)^2\right)\frac{dz}{z^2}$
Málaga	$A\sum_{m=1}^{\beta}a_m\exp\left(\frac{\alpha+m}{2}x\right)K_{\alpha-m}\left(2\sqrt{\frac{\alpha\beta\exp(x)}{g\beta+\Omega_0}}\right)$
Double Generalized Gamma	$\frac{\alpha_2\lambda\sigma^{\beta_1-\frac{1}{2}}\lambda^{\beta_2-\frac{1}{2}}(2\pi)^{1-\frac{\sigma+\lambda}{2}}}{\Gamma(\beta_1)\Gamma(\beta_2)}G_{\lambda+\sigma,0}^{0,\lambda+\sigma}\left[\frac{(\Omega_2\lambda)^\lambda(\sigma\Omega_1)^\sigma}{\beta_1^\sigma\beta_2^\lambda\exp(\alpha_2\lambda x)}\middle\vert\begin{matrix}1-\kappa_0\\-\end{matrix}\right]$

$$f_{y_p}(x)=\frac{w_{zeq}^2}{8\pi\sigma_x\sigma_y}\int_0^{2\pi}\exp\left(-\left(\xi_x\cos(\phi)\sqrt{\log(A_0)-x}-\frac{\mu_x}{\sqrt{2}\sigma_x}\right)^2-\left(\xi_y\sin(\phi)\sqrt{\log(A_0)-x}-\frac{\mu_y}{\sqrt{2}\sigma_y}\right)^2\right)d\phi. \quad (15)$$

where $\alpha = 1.96$. The efficiency indicator of IS method compared to MC is defined as [33]

$$G=\frac{N}{N^*}=\frac{P_{\text{out}}(1-P_{\text{out}})}{\text{Var}^*[\mathbb{1}_{(y_a+y_p<\varepsilon)}\omega_{y_a}(y_a)\omega_{y_p}(y_p)]}. \quad (22)$$

B. Exponential Twisting

Exponential twisting technique, also known as exponential tilting or change in exponential measure [34]-[35], is well known in IS and is particularly used for its properties on the sums of random variables. The method is based on the theory of large deviations [36]. The main idea is to define the auxiliary density $f^*(\cdot)$ as

$$f_{y_k}^*(y)=\frac{e^{\theta y}}{\mathcal{M}_{y_k}(\theta)}f_{y_k}(y),\ k\in\{a,p\}, \quad (23)$$

where $\mathcal{M}_{y_k}(\theta)=\mathbb{E}[e^{\theta y_k}]$ is the MGF of y_k. In this case, the weighting function is given by

$$\omega_{y_k}(y,\theta)=e^{-\theta y}\mathcal{M}_{y_k}(\theta). \quad (24)$$

Note that the biased PDF depends on the parameter θ. In order to minimize the variance of IS estimator, the quantity $\mathbb{E}^*[\mathbb{1}^2_{(y_a+y_p<\varepsilon)}\omega_a^2(y_a,\theta)\omega_{y_p}^2(y_p,\theta)]$ needs to be minimized w.r.t the parameter θ as discussed in the next subsection. Since we are interested in estimating a left tail probability, the value of θ needs to be negative.

The MGFs of y_a for the different turbulence regimes is given in Table II, where ${}_1F_1(\cdot,\cdot,\cdot)$ represents the confluent hypergeometric F function [29, Eq. (9.210.1)]. For the pointing errors, it can be shown, after some manipulations, that the MGF of y_p is given by

$$\mathcal{M}_{y_p}(\theta)=\mathbb{E}[h_p^\theta]=\frac{\xi_x\xi_y A_0^\theta\exp\left(-\frac{2\theta}{w_{zeq}^2}\left[\frac{\mu_x^2\xi_x^2}{\xi_x^2+\theta}+\frac{\mu_y^2\xi_y^2}{\xi_y^2+\theta}\right]\right)}{\sqrt{(\xi_x^2+\theta)(\xi_y^2+\theta)}}. \quad (25)$$

For the lognormal case, the MGF is derived using the fact that y_a is a Gaussian RV with mean $-\frac{\sigma_R^2}{2}$ and variance σ_R^2. The derivation of the MGF of y_a in the Rician-lognormal, Málaga, and Double Generalized Gamma turbulence cases can be found in Appendix A. For the pointing errors, substituting $y_p=\log(A_0)-\frac{2r^2}{w_{zeq}^2}$, and using the MGF of r^2 given in [37, Eq. (2.38)], we get (25).

C. Optimization Algorithm

To determine the optimal θ^*, we need to solve the following minimization problem

$$\min_{\theta\in\mathbb{R}} J(\theta)=\mathbb{E}^*[\mathbb{1}_{(y_a+y_p<\varepsilon)}\omega_{y_a}^2(y_a,\theta)\omega_{y_p}^2(y_p,\theta)]. \quad (26)$$

Not only that this problem can be seen as a random optimization problem, but it also is usually not feasible analytically to solve, except for a few simple cases. In [18], the author derives an upper bound for the second moment, using ideas similar to the Chernoff bound derivation. By optimizing this bound, a sub-optimal solution can be found that guarantees a gain slightly less than the one using the optimal value. The advantage of using this approach lies in the fact that it just requires solving the deterministic problem

$$\mu'(\theta)=\varepsilon, \quad (27)$$

where $\mu'(\cdot)$ is the derivative of the cumulant generating function (CGF) of the RV (y_a+y_p), i.e. $\mu(\theta)=\log(\mathbb{E}[e^{\theta(y_a+y_p)}])$. To find this sub-optimal θ, we show in Appendix B, that we need to solve (41)-(44) for Lognonormal, Rician-Lognormal, Málaga, and Double Generalized Gamma turbulence models, respectively, where $\psi(x)=\frac{\Gamma'(x)}{\Gamma(x)}$ is the digamma function and

$${}_1F_1{}^{(1,0,0)}[a;b;z]=\frac{z}{b}\ F_{2\times0\times1}^{1\times1\times2}\left(\begin{matrix}a+1;1;1,a;\\2,b+1;;a+1;\end{matrix}z,z\right), \quad (28)$$

where $F_{2\times0\times1}^{1\times1\times2}(\cdot)$ is the Kampé de Fériet-like function [38]. Solving these equations results in a set of solutions. We choose a real solution, such that the MGFs are well defined, to be the sub-optimal solution.

Remark 1. *Eq. (27) needs to be solved in the domain of definition of the CGF of the turbulence PDF assumed. In the case a solution does not exist in this domain, we can either*

- *consider the solution θ that gives the minimum value for the absolute difference $|\mu'(\theta)-\varepsilon|$ or,*
- *use another method to characterize θ. For instance, we can use the cross-entropy method [39, Sec. 9.7.3] or the*

This article has been accepted for publication in a future issue of this journal, but has not been fully edited. Content may change prior to final publication. Citation information: DOI 10.1109/TWC.2017.2731947, IEEE Transactions on Wireless Communications

TABLE II: MGF of y_a for different turbulence regimes.

Turbulence model	**MGF of y_a : $\mathcal{M}_{y_a}(\theta) = \mathbb{E}[h_a^\theta]$**	**Conditions on θ**
Lognormal	$\exp\left(\frac{1}{2}\theta(\theta-1)\sigma_R^2\right)$	
Rician-Lognormal	$\left(\frac{\Omega}{1+k^2}\right)^\theta \Gamma(1+\theta)\ \exp\left(\frac{1}{2}\theta(\theta-1)\sigma_R^2\right)\ {}_1F_1(-\theta,1,-k^2)$	$\theta > -1$
Málaga	$\frac{A}{2}\Gamma(\theta+\alpha)\sum_{m=1}^{\beta} a_m \left(\frac{g\beta+\Omega_0}{\alpha\beta}\right)^{\frac{\alpha+m}{2}+\theta}\Gamma(\theta+m)$	$\theta > -\min(1,\alpha)$
Double Generalized Gamma	$\left(\frac{\Omega_1}{\beta_1}\right)^{\frac{\theta}{\alpha_1}}\left(\frac{\Omega_2}{\beta_2}\right)^{\frac{\theta}{\alpha_2}}\frac{\Gamma\left(\beta_1+\frac{\theta}{\alpha_1}\right)\Gamma\left(\beta_2+\frac{\theta}{\alpha_2}\right)}{\Gamma(\beta_1)\Gamma(\beta_2)}$	$\theta > -\min(\alpha_1\beta_1,\alpha_2\beta_2)$

stochastic counterpart method [39, Sec. 12.2] to find θ that minimizes the second moment of the IS estimator.

D. Sampling Method

To sample from the biased PDF $f^*(\cdot)$ may not be very trivial, especially when the new PDF does not resemble a known parametric PDF. In this case, we can use standard techniques such as the inverse transformation method or the acceptance-rejection technique [40, Sec. 2.2, 2.3].

For the sampling from the biased PDF in the case of lognormal turbulence, we show in Appendix C that we can use the inverse CDF method. In fact, in our particular case, it can be shown, after some mathematical manipulations, that the inverse CDF, is given by

$$[F^*_{y_a}]^{-1}(u) = \sigma_R\left(\sqrt{2}\ \text{erf}^{-1}(2u-1) - (\frac{1}{2}-\theta)\sigma_R\right), \quad (29)$$

where the error function is defined as $\text{erf}(x) = \frac{2}{\sqrt{\pi}}\int_0^x e^{-t^2}dt$. The inverse error function $\text{erf}^{-1}(\cdot)$ can be called in MATLAB for instance, using the function `erfinv`.

For the sampling from the twisted PDFs of the other turbulence models as well as the pointing errors, it is difficult to find an explicit expression for the inverse CDF. An interesting alternative is to approximate the inverse CDF, instead of finding its expression analytically. In [41], an efficient method for sampling from one-dimensional PDFs is developed. The method is based on approximating the inverse CDF using Chebyshev polynomials. The authors show the robustness of the method against other techniques, such as slice sampling and rejection sampling. A MATLAB implementation of this method is available in [42]. For readability purpose, we have included the sampling algorithm from [41] in Appendix D.

E. Correlated Sways

So far in this paper, we assume that the horizontal and vertical displacement of the beam, r_x and r_y, are independent. However, this assumption can be relaxed and our approach is still valid for this kind of problem. In fact, let $r_x \sim \mathcal{N}(\mu_x, \sigma_x^2)$ and $r_y \sim \mathcal{N}(\mu_y, \sigma_y^2)$ be two correlated Gaussian RVs with a Pearson correlation coefficient $\rho \in [-1, 1]$. Inspired by the whitening approach proposed recently in [43], we can find $r'_x \sim \mathcal{N}(\mu'_x, {\sigma'_x}^2)$ and $r'_y \sim \mathcal{N}(\mu'_y, {\sigma'_y}^2)$ two independent Gaussian RVs such that $r^2 = {r'_x}^2 + {r'_y}^2$. The latter equation presents the case treated in this work. In [43], the authors approximated the Beckmann distribution by a modified Rayleigh distribution. Based on this approximation, they studied the outage performance over Gamma-Gamma fading channels. The novelty of our work compared to [43] is that we are considering a general distribution for the pointing error based on Beckmann distribution.

The parameters of the distribution of r'_x and r'_y can be expressed as [43]

$$\begin{cases} \mu'_x &= \mu_x\cos\phi_0 + \mu_y\sin\phi_0 \\ \mu'_y &= \mu_y\cos\phi_0 - \mu_x\sin\phi_0 \\ {\sigma'_x}^2 &= \sigma_x^2\cos^2\phi_0 + \sigma_y^2\sin^2\phi_0 + 2\rho\sigma_x\sigma_y\sin\phi_0\cos\phi_0 \\ {\sigma'_y}^2 &= \sigma_y^2\cos^2\phi_0 + \sigma_x^2\sin^2\phi_0 - 2\rho\sigma_x\sigma_y\sin\phi_0\cos\phi_0 \end{cases} \quad (30)$$

where the expression of ϕ_0 is given by [43]

$$\phi_0 = \begin{cases} \frac{\pi}{4}, & \text{if } \sigma_x = \sigma_y \\ \frac{1}{2}\arctan\left(\frac{2\rho\sigma_x\sigma_y}{\sigma_x^2-\sigma_x{y}^2}\right), & \text{otherwise} \end{cases} \quad (31)$$

IV. Multihop systems

After explaining the basic ideas behind our approach in the single hop case, we show in this section how to extend these ideas to estimate bounds for the outage probability in the case of multihop systems. First, we recall briefly the system model and then we show the flexibility of the proposed approach to tackle the multihop scenario. The end-to-end SNR of N-hop systems can be written as [17]

$$\gamma_{end} \triangleq \left(\sum_{i=1}^{N}\frac{1}{\gamma_i}\right)^{-1}. \quad (32)$$

In this work, we assume that the hops undergo independent turbulence influence. In the case FSO systems with CSI-assisted relays, γ_{end} can be upper bounded by [44]

$$\gamma_{end} \leq \gamma_{sub} = \frac{1}{N}\prod_{i=1}^{N}\gamma_i^{\frac{1}{N}}. \quad (33)$$

Since we have $\gamma_{end} \leq \gamma_{sub}$, then we can write $F_{\gamma_{sub}}(\gamma_{th}) = \mathbb{P}(\gamma_{sub} \leq \gamma_{th}) \leq P_{out}$. Using the definition of γ_{sub}, we have

$$\begin{aligned} F_{\gamma_{sub}}(\gamma_{th}) &= \mathbb{P}\left(\frac{1}{N}\prod_{i=1}^{N}\gamma_i^{\frac{1}{N}} \leq \gamma_{th}\right), \\ &= \mathbb{P}\left(\prod_{i=1}^{N}\gamma_i \leq (N\gamma_{th})^N\right). \end{aligned} \quad (34)$$

Since we have $\gamma_i = \gamma_0 h_i^2$, the expression of the CDF of γ_{sub} becomes

$$F_{\gamma_{sub}}(\gamma_{th}) = \mathbb{P}\left(\prod_{i=1}^{N}h_i \leq \left(\frac{N\gamma_{th}}{\gamma_0}\right)^{\frac{N}{2}}\right). \quad (35)$$

This article has been accepted for publication in a future issue of this journal, but has not been fully edited. Content may change prior to final publication. Citation information: DOI 10.1109/TWC.2017.2731947, IEEE Transactions on Wireless Communications

Assuming each fading channel h_i can be written as $h_i = h_l h_{a,i} h_{p,i}$, we obtain

$$F_{\gamma_{sub}}(\gamma_{th}) = \mathbb{P}\left(\prod_{i=1}^{N} h_{a,i}h_{p,i} \leq \left(\frac{N\gamma_{th}}{h_l^2\gamma_0}\right)^{\frac{N}{2}}\right), \quad (36)$$

$$= \mathbb{P}\left(\sum_{i=1}^{N}(y_{a,i} + y_{p,i}) \leq \epsilon\right), \quad (37)$$

where $y_{a,i} = \log(h_{a,i})$, $y_{p,i} = \log(h_{p,i})$, $1 \leq i \leq N$ and $\epsilon = \frac{N}{2}\log\left(\frac{N\gamma_{th}}{h_l^2\gamma_0}\right)$. Here, $y_{a,i}$ follows one of the PDFs of Table I while $y_{p,i}$ follows the PDF (15).

Now, we explain briefly how to extend the approach developed in the single hop case for the estimation of $F_{\gamma_{sub}}(\gamma_{th})$. The naive MC estimator is given by

$$\mathrm{I} = \frac{1}{N}\sum_{n=1}^{N} \mathbb{1}_{(S_{N,n}<\varepsilon)}, \quad (38)$$

where $S_N = \sum_{i=1}^{N}(y_{a_i} + y_{p_i})$ and $y_{a_i,n}$ and $y_{p_i,n}$ from the original PDFs $f_{y_{a_i}}(\cdot)$ and $f_{y_{p_i}}(\cdot)$, respectively. Inspired by the single hop scenario, the IS estimator is thereby

$$\mathrm{I}^* = \frac{1}{N^*}\sum_{n=1}^{N^*} \mathbb{1}_{(S^*_{N,n}<\varepsilon)} \prod_{i=1}^{N} \omega_{y_{a_i}}(y^*_{a_i,n})\omega_{y_{p_i}}(y^*_{p_i,n}), \quad (39)$$

where $y^*_{a_i,n}$ and $y^*_{p_i,n}$ are here sampled from the biased PDFs $f^*_{y_{a_i}}(\cdot)$ and $f^*_{y_{p_i}}(\cdot)$, respectively and the likelihood functions are given by

$$\omega_{y_{k_i}}(y) = \frac{f_{y_{k_i}}(y)}{f^*_{y_{k_i}}(y)},\ k \in \{a,p\},$$

$$= e^{-\theta y}\mathcal{M}_{y_{k_i}}(\theta),\ k \in \{a,p\}, \quad (40)$$

where $\mathcal{M}_{y_{k_i}}(\theta) = \mathbb{E}[e^{\theta y_{k_i}}]$ is the MGF of y_{k_i}.

To find the suboptimal θ, we solve the problem $\mu'_N(\theta) = \varepsilon$, where $\mu_N(\theta) = \log(\mathbb{E}[e^{\theta S_N}])$. Let n_L, n_{RL}, n_M, and n_D, such that $n_L + n_{RL} + n_M + n_D = N$, denote the number of hops where h_a follows Lognormal, Rician-Lognormal, Málaga, and Double Generalized Gamma turbulence model, respectively. Then, the optimization problem reduces to finding the solution of the equation (45) where $\mu_{y_{a_i,L}}(\cdot)$, $\mu_{y_{a_i,RL}}(\cdot)$, $\mu_{y_{a_i,M}}(\cdot)$, $\mu_{y_{a_i,D}}(\cdot)$, and $\mu_{y_{p_i}}(\cdot)$ denote the CGF of Lognormal, Rician-Lognormal, Málaga, Double Generalized Gamma and pointing error models, respectively.

Remark 2. *In our work, we are considering a non regenerative AF system. In this case, the end-to-end SNR of N-hop systems can be written as*

$$\gamma_{end} \triangleq \left(\sum_{i=1}^{N}\frac{1}{\gamma_i}\right)^{-1}, \quad (46)$$

whereas for regenerative system, the expression of the end-to-end SNR is given by

$$\gamma_{end} \triangleq \min_{1\leq i\leq N}\gamma_i. \quad (47)$$

In this case, the analysis becomes different and the derivation done in this work are no longer valid. For the repositioning, we consider the analysis for a fixed multihop configuration. If the configuration is modified, the analysis is still valid, however we need to take into account that the parameters of simulations are no longer the same.

V. Numerical Simulations

Table III summarizes the system settings used in this section. Table IV details the system parameters under different turbulence conditions. These parameters have been used in the study of many FSO systems, for instance [5], [10], [45], and [32].

TABLE III: System parameters.

Parameters	Value
Receiver radius (a)	10 cm
Noise standard deviation (σ_n)	10^{-7} A/Hz
Beam radius (ω_z)	100 cm
Horizontal jitter standard deviation (σ_x)	10 cm
Vertical jitter standard deviation (σ_y)	20 cm
Horizontal jitter mean (μ_x)	10 cm
Vertical jitter mean (μ_y)	5 cm

In this section, we dedicate the first part to show the efficiency of IS compared to standard MC in the single hop case. The second part deals with the study of the difference of horizontal and vertical jitter effects (i.e. the building may sway differently in the horizontal plane than in the vertical plane) on the outage probability. Finally, we show simulation results for the case of multihop systems.

A. Validation of our Approach

The behavior of the outage probability, as a function of the average transmitted optical power P_t is depicted in Fig. 1a for the lognormal turbulence, in Fig. 1b for the Rician-Lognormal scenario, in Fig. 1d for the Málaga case, and Fig. 1c for the Double Generalized Gamma. These figures are plotted using 10^5 samples for IS and 10^8 samples for MC. For relatively high values of probabilities, the standard MC matches the IS method and provides a very accurate approximation for the outage probability. However, for small probabilities, our approach can accurately estimate the outage probability with $N^* = 10^5$ while the standard MC fails and can give an erroneous estimation in spite of using $N = 10^8$ samples. To achieve the same accuracy, the number of samples of MC needs to be increased. For each type of turbulence, we provide simulations for two set of parameters to validate our approach for different degrees of turbulence severity.

To have a clear look at the efficiency of IS, we turn our attention to Table V where we examine the efficiency indicator defined in (22). This table presents the IS gain for different turbulence models and different parameters. This metric measures the reduction in terms of number of samples needed and is based on the ratio of the variances of the two estimators. We note that the efficiency indicator grows as the outage probability becomes smaller, which means that the method becomes more efficient in the low outage probability region. For instance, in the lognormal turbulence when $\sigma_R^2 = 0.05$, for P_{out} of the order of 10^{-6}, the gain in number of samples

This article has been accepted for publication in a future issue of this journal, but has not been fully edited. Content may change prior to final publication. Citation information: DOI 10.1109/TWC.2017.2731947, IEEE Transactions on Wireless Communications

$$\log(A_0) + \frac{\sigma_R^2}{2}(2\theta - 1) - \frac{\xi_x^2 + \xi_y^2 + 2\theta}{2(\xi_x^2 + \theta)(\xi_y^2 + \theta)} - \frac{2}{w_{zeq}^2}\left[\frac{\mu_x^2\xi_x^4}{(\xi_x^2 + \theta)^2} + \frac{\mu_y^2\xi_y^4}{(\xi_y^2 + \theta)^2}\right] = \varepsilon, \tag{41}$$

$$\log\left(\frac{A_0\Omega}{1+k^2}\right) - \frac{\xi_x^2 + \xi_y^2 + 2\theta}{2(\xi_x^2 + \theta)(\xi_y^2 + \theta)} - \frac{2}{w_{zeq}^2}\left[\frac{\mu_x^2\xi_x^4}{(\xi_x^2 + \theta)^2} + \frac{\mu_y^2\xi_y^4}{(\xi_y^2 + \theta)^2}\right] + \frac{\sigma_R^2}{2}(2\theta - 1) + \psi(\theta + 1) - \frac{{}_1F_1^{(1,0,0)}(-\theta, 1, -k^2)}{{}_1F_1(-\theta, 1, -k^2)} = \varepsilon, \tag{42}$$

$$\log(A_0) - \frac{\xi_x^2 + \xi_y^2 + 2\theta}{2(\xi_x^2 + \theta)(\xi_y^2 + \theta)} - \frac{2}{w_{zeq}^2}\left[\frac{\mu_x^2\xi_x^4}{(\xi_x^2 + \theta)^2} + \frac{\mu_y^2\xi_y^4}{(\xi_y^2 + \theta)^2}\right] + \psi(\theta + \alpha) + \log\left(\frac{g\beta + \Omega_0}{\alpha\beta}\right) + \frac{\sum_{m=1}^{\beta} a_m \left(\frac{g\beta+\Omega_0}{\alpha\beta}\right)^{\frac{\alpha+m}{2}+\theta} \Gamma(\theta + m)\ \psi(\theta + m)}{\sum_{m=1}^{\beta} a_m \left(\frac{g\beta+\Omega_0}{\alpha\beta}\right)^{\frac{\alpha+m}{2}+\theta} \Gamma(\theta + m)} = \varepsilon, \tag{43}$$

$$\log(A_0) - \frac{\xi_x^2 + \xi_y^2 + 2\theta}{2(\xi_x^2 + \theta)(\xi_y^2 + \theta)} - \frac{2}{w_{zeq}^2}\left[\frac{\mu_x^2\xi_x^4}{(\xi_x^2 + \theta)^2} + \frac{\mu_y^2\xi_y^4}{(\xi_y^2 + \theta)^2}\right] + \frac{\log\left(\frac{\Omega_1}{\beta_1}\right) + \psi\left(\beta_1 + \frac{\theta}{\alpha_1}\right)}{\alpha_1} + \frac{\log\left(\frac{\Omega_2}{\beta_2}\right) + \psi\left(\beta_2 + \frac{\theta}{\alpha_2}\right)}{\alpha_2} = \varepsilon. \tag{44}$$

$$\sum_{i=1}^{n_L} \mu'_{y_{a_i,L}}(\theta) + \sum_{i=1}^{n_{RL}} \mu'_{y_{a_i,RL}}(\theta) + \sum_{i=1}^{n_M} \mu'_{y_{a_i,M}}(\theta) + \sum_{i=1}^{n_D} \mu'_{y_{a_i,D}}(\theta) + \sum_{i=1}^{N} \mu'_{y_{p_i}}(\theta) = \varepsilon, \tag{45}$$

TABLE IV: System characteristics under different weather conditions.

Turbulence Severity	Path loss (h_l)	Fading Model	Parameters
Weak turbulence	0.008	Lognormal	$\sigma_R^2 = 0.05$
			$\sigma_R^2 = 0.2$
		Rician-Lognormal	$k = 2$
			$k = 3$
Moderate to strong turbulence	0.9	Malaga	$\alpha = 2.296$, $\beta = 2$
			$\alpha = 4.2$, $\beta = 3$
		Double Generalized Gamma	Case 1: $\beta_1 = 0.5$, $\beta_2 = 1.8$, $\alpha_1 = 1.8621$, $\alpha_2 = 1$, $\Omega_1 = 1.5074$, $\Omega_2 = 1$
			Case 2: $\beta_1 = 0.55$, $\beta_2 = 2.35$, $\alpha_1 = 2.169$, $\alpha_2 = 1$, $\Omega_1 = 1.5793$, $\Omega_2 = 1$

is of the order of 10^4. The second metric used to compare the two methods, in this paper, is the relative error defined in (21). It gives us an idea regarding the confidence interval of the estimated parameter. In fact, the relative error is defined as the ratio of half of the confidence interval width over the value estimated. This comparison is reported in Fig. 2, when $N^* = 10^4$ and $N = 10^6$, for the lognormal, Rician-lognormal, Málaga, and Double Generalized Gamma turbulence scenarios, respectively. We consider the case when $\sigma_R^2 = 0.05$ for the lognormal turbulence, $k = 3$ for the Rician-lognormal, ($\alpha = 2.296$, $\beta = 2$) for the Málaga scenario, and ($\beta_1 = 0.55$, $\beta_2 = 2.35$, $\alpha_1 = 2.169$, $\alpha_2 = 1$, $\Omega_1 = 1.5793$, $\Omega_2 = 1$) for the Double Generalized Gamma case. It is clear that the variation of the relative error of the IS is much slower than that of standard MC. We note also, that for low outage probability, the relative error of IS is smaller than standard MC, although the number of samples used for MC is 100 times greater than the one used for IS simulation.

B. Impact of the Difference of Jitter Effects on Outage Probability

One of the aims of the paper is to be able to study the impact of the difference of jitter effects on the outage probability. To this end, we use the IS method developed in section III. The difference of jitter effects can take place in real life when the intensity of the motion of the building in the vertical direction is different from the horizontal direction. To quantify this effect, we can, for instance, compare the outage probability for the FSO system when we have the same jitter standard deviation, to the case when the horizontal jitter standard deviation is different from the vertical one. Fig. 3a reports the results under lognormal turbulence while the outage probability under Rician-lognormal turbulence is depicted by Fig. 3b. The impact of the difference of jitter effects on the outage probability for Málaga, and Double Generalized Gamma turbulence is presented in Figs. 3d-3c. In these plots, we choose to change the jitter standard deviation

This article has been accepted for publication in a future issue of this journal, but has not been fully edited. Content may change prior to final publication. Citation information: DOI 10.1109/TWC.2017.2731947, IEEE Transactions on Wireless Communications

TABLE V: Efficiency indicator under different turbulence models.

Turbulence Model	Parameters	IS Gain ($\times 10^3$)			
Lognormal	P_t (dBm)	3	5	7	9
	$\sigma_R^2 = 0.05$	0.2	3.4	62.8	106.9
	$\sigma_R^2 = 0.2$	0.02	0.06	0.22	0.83
Rician-Lognomal	P_t (dBm)	41	43	45	47
	$k = 2$	9.9	14.9	25.5	38.3
	$k = 3$	34.5	57.1	93.1	125
Málaga	P_t (dBm)	31	33	35	37
	$\alpha = 2.296$, $\beta = 2$	45.5	70.1	103.5	167.4
	$\alpha = 4.2$, $\beta = 3$	99.5	118.4	285.9	414.6
Double Generalized Gamma	P_t (dBm)	31	33	35	37
	Case 1	4.9	7.7	11.2	16.5
	Case 2	29.1	47.9	67.6	98.4

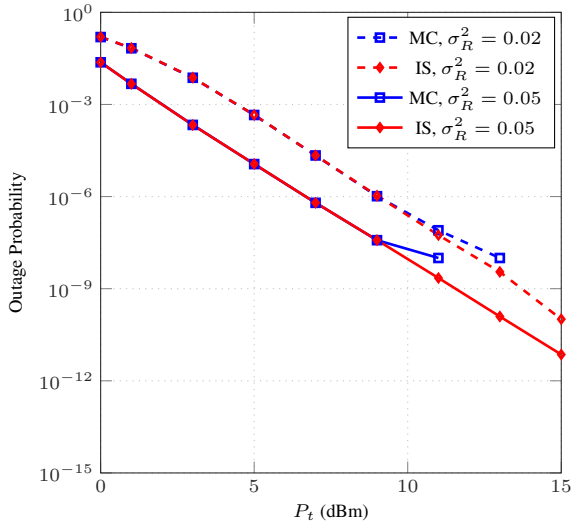

(a) Lognormal turbulence.

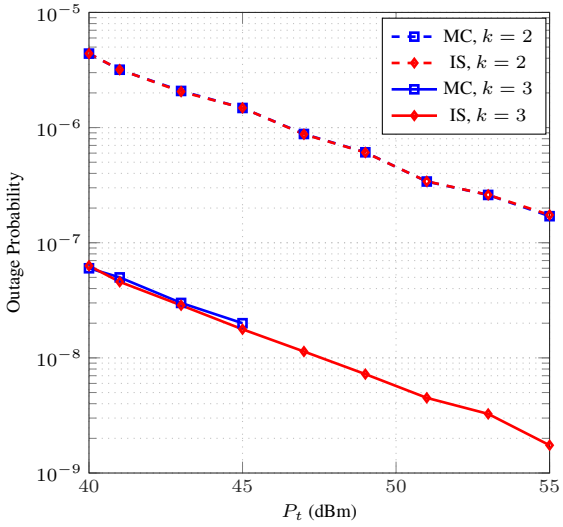

(b) Rician-Lognormal turbulence.

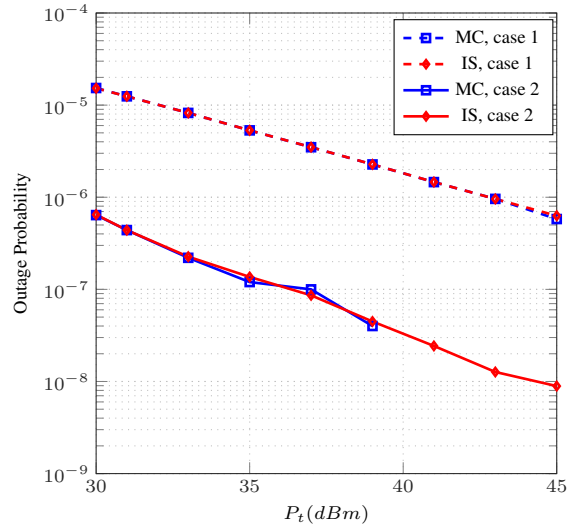

(c) Double Generalized Gamma turbulence.

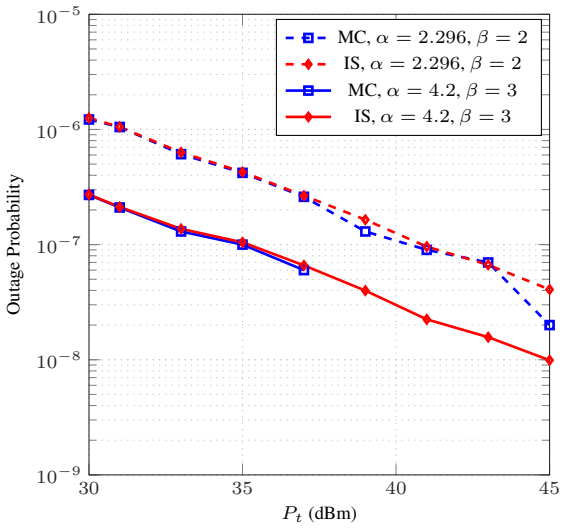

(d) Málaga turbulence.

Fig. 1: Outage probability with $N^* = 10^5$ and $N = 10^8$ with general pointing errors.

in the vertical direction while maintaining the jitter standard deviation in the horizontal direction fixed. Note that as the vertical jitter standard deviation σ_y increases, i.e. the vibration of the building is more intense in the vertical direction, the outage probability tends to increase significantly.

C. Effect of the Severity and Type of Turbulence

In this section, we investigate the effect of the severity of the turbulence on the outage probability of FSO links under the same pointing error conditions. In Fig. 4, we plot the outage probability under three different turbulence regimes: weak

This article has been accepted for publication in a future issue of this journal, but has not been fully edited. Content may change prior to final publication. Citation information: DOI 10.1109/TWC.2017.2731947, IEEE Transactions on Wireless Communications

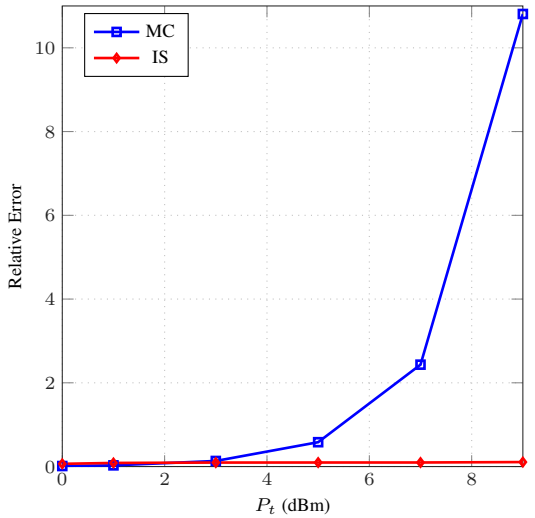

(a) Lognormal turbulence with $\sigma_R^2 = 0.05$.

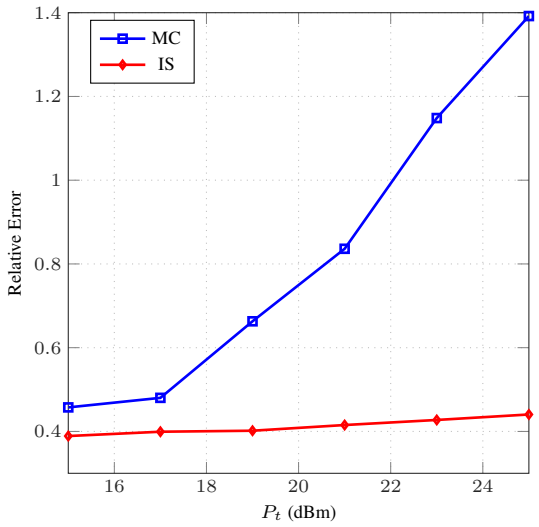

(b) Rician-Lognormal turbulence with $k = 3$.

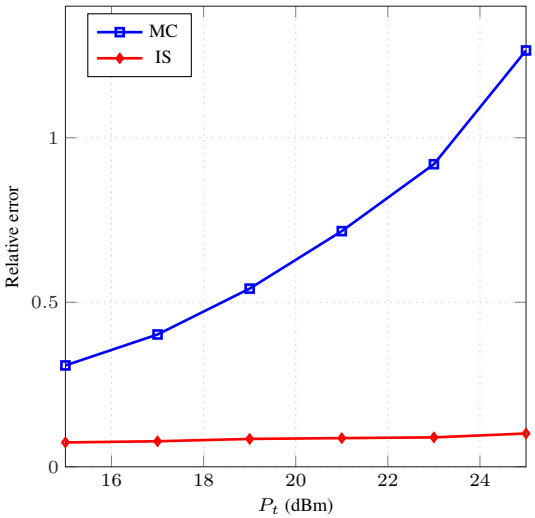

(c) Double Generalized Gamma turbulence (case 2 parameters).

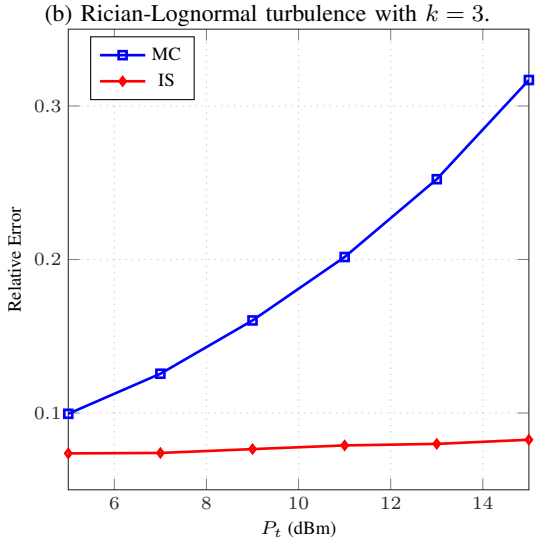

(d) Málaga turbulence with $\alpha = 2.296$ and $\beta = 2$.

Fig. 2: Relative error with $N^* = 10^4$ and $N = 10^6$.

turbulence modeled by lognormal distribution as a special case of the Málaga turbulence model, moderate turbulence when the atmospheric turbulence is modeled by the Double Generalized Gamma, and the strong turbulence when the Málaga turbulence model is assumed. We can clearly see that as the turbulence becomes stronger, the outage probability becomes greater and thus the performance of the system deteriorates. A comparison between the lognormal and Rician-lognormal turbulence models is reported in Fig. 5. In this plot, we see that as k becomes bigger the Rician-lognormal model approaches the lognormal one. As $k \to +\infty$, the Rician effect becomes negligible and the Rician-lognormal case reduces the lognormal scenario.

D. Multihop System

In this section, we present some selected simulation results illustrating how our approach works to the multihop case. In Fig. 6, we plot the bounds of the outage probability for three scenarios

(i) The top plot is for the case when the number of hops is $N = 10$. For each hop, we consider the same model where we assume that the fading model follows the Double Generalized Gamma with parameters of the case 2 detailed in Table IV,
(ii) The middle plot is for the same case as (i) but with a number of hops $N = 3$,
(iii) The bottom plot represents the scenario when we have $N = 3$ hops with different fading models (Lognormal, Málaga, and Double Generalized Gamma).

In all the three cases, we assume that the pointing error has the parameters of Table III in each hop. We also assume that the length of each hop is the same for the three scenarios, thus the total distance between the transmitter and the receiver is not the same. As can be seen from the plot, both naive MC and IS matches. However, IS provide a significant reduction in term of number of samples especially when the probability to be estimated is very small. For instance, in the bottom plot (case (iii)), the gain factor, when the probability is of

This article has been accepted for publication in a future issue of this journal, but has not been fully edited. Content may change prior to final publication. Citation information: DOI 10.1109/TWC.2017.2731947, IEEE Transactions on Wireless Communications

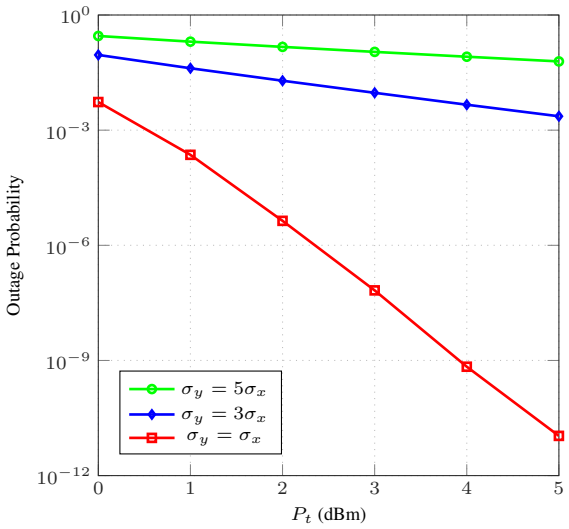

(a) Lognormal turbulence with $\sigma_R^2 = 0.05$.

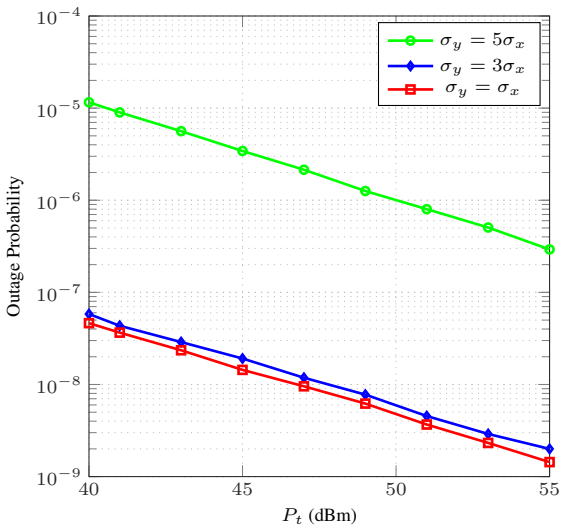

(b) Rician-Lognormal turbulence with $k = 3$.

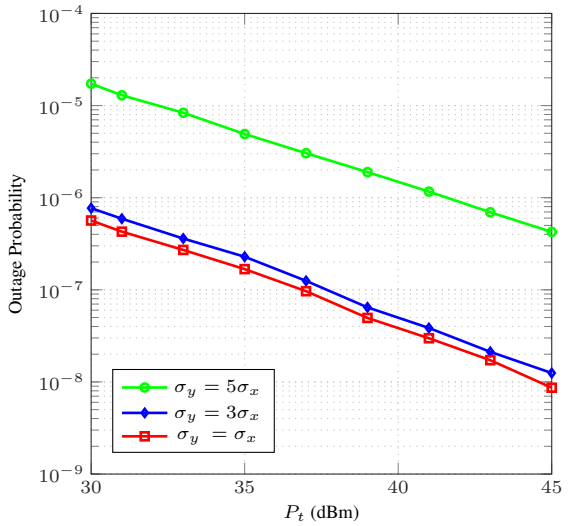

(c) Double Generalized Gamma turbulence using case 2 parameters.

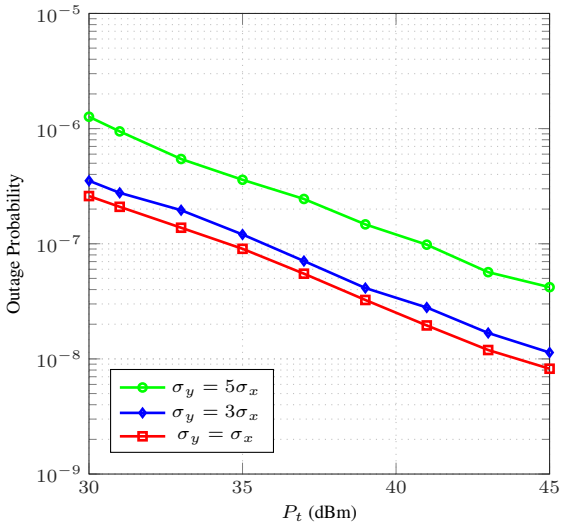

(d) Málaga turbulence with $\alpha = 4.2$ and $\beta = 3$.

Fig. 3: Impact of the difference of jitter effects on outage probability under different turbulence conditions.

the order of 10^{-5}, is of the order of 10^3 while it becomes of the order of 10^5 when the probability reaches 10^{-7}. In addition to that, we can see that while naive MC matches IS for high values of outage probabilities, its accuracy when using $N = 10^8$ samples worsen as the outage probability becomes smaller. Unless more samples are taken in this region, naive MC remains unable to accurately estimate the outage probability.

In Fig. 7, we plot the bounds of the outage probabilities of multihop systems under Gamma-Gamma turbulence fading for three different numbers of hops $N \in \{1, 2, 4\}$. The distance between the transmitter and the receiver is fixed in this case $z = 5$km and we assume that the pointing error conditions are the same for the three scenarios. We notice that when the number of hops increases, the performance of the system becomes better. For instance, for $P_t = -15$ dBm, the outage probability when using a single hop is 0.098 whereas it is of the order of 2×10^{-7} when using $N = 4$ hops. For the comparison between standard MC and IS, we can draw similar conclusions as in Fig. 6. In fact, MC is sufficient for the estimation of relatively high probabilities (greater than 10^{-5}), however it fails completely when these probabilities become in the rare event region, unless more samples are considered. IS with only $N^* = 10^5$ is able to estimate probabilities of the order of 10^{-15} (case when $N = 4$) unlike standard MC with $N = 10^8$. The efficiency of IS compared to MC can be seen by examining the gain factor G. The latter is of the order of 5×10^3 for $N = 2$ when $P_t = -11$ dBm, and of the order of 10^9 when $N = 4$ for $P_t = -13$ dBm. Thereby, we can see that the proposed approach results in a significant reduction in terms of the number of samples especially when the outage probability is very small.

VI. Conclusion

In this work, we have introduced an exponential twisting-based IS approach to estimate the outage probability of single

This article has been accepted for publication in a future issue of this journal, but has not been fully edited. Content may change prior to final publication. Citation information: DOI 10.1109/TWC.2017.2731947, IEEE Transactions on Wireless Communications

hop as well as multihop FSO systems under generalized pointing errors in the presence of different turbulence regimes. The comparison of the performance of the IS approach to standard MC shows a significant reduction in the number of simulation runs for the same level of accuracy especially in the region of very small outage probability. We also investigated the impact of the severity of the turbulence as well as the difference of jitter effects on the outage probability. Based on selected simulation results, we have notice that as the jitter effect increases in a particular direction or the atmospheric turbulence becomes stronger, the outage probability tends to increase significantly.

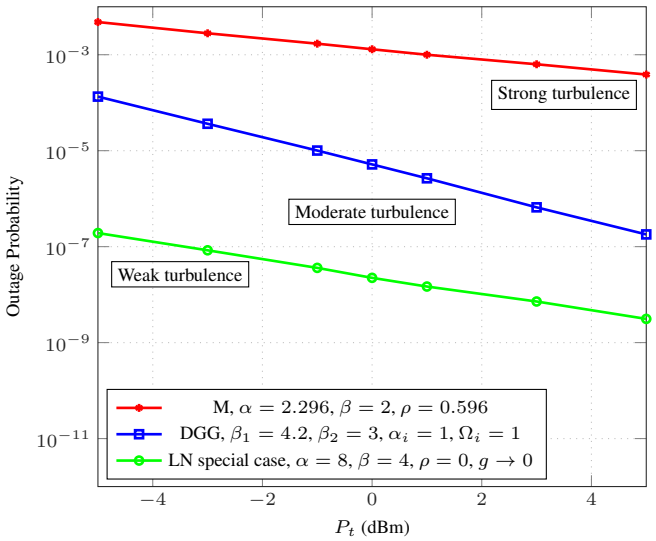

Fig. 4: Outage probability under different turbulence models.

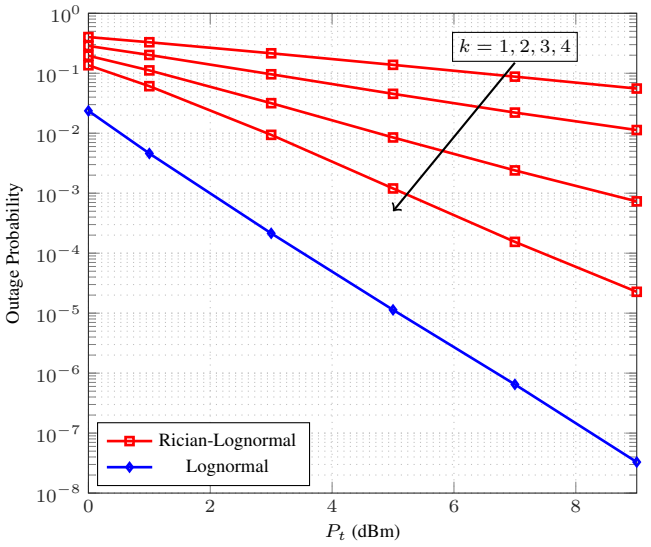

Fig. 5: Outage probability under lognormal and Rician-lognormal turbulence with varying Rician parameter k.

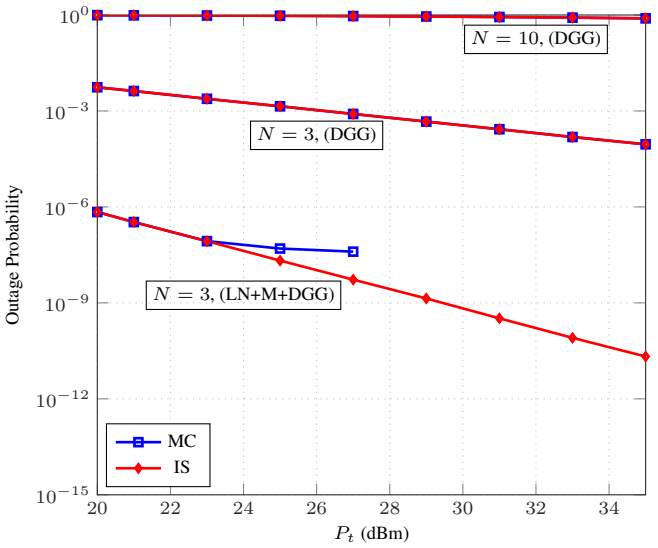

Fig. 6: Outage probability bounds for multihop system.

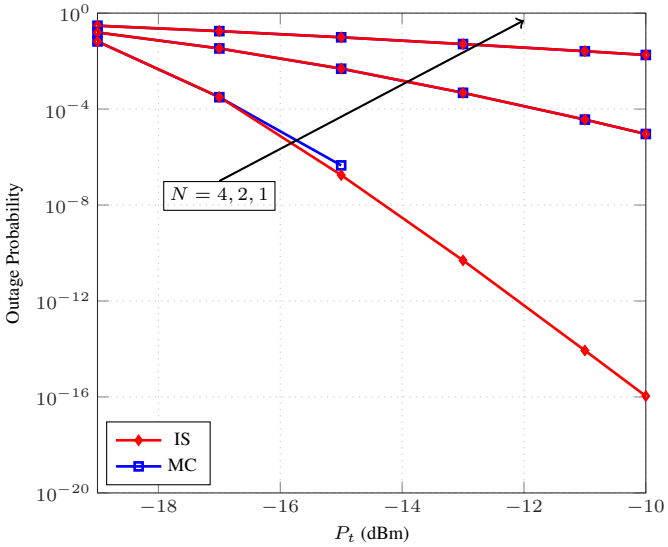

Fig. 7: Outage probability bounds for multihop systems under Gamma-Gamma turbulence.

APPENDIX A
MGF OF y_a FOR DIFFERENT TURBULENCE MODELS

A. Rician-lognormal Turbulence

In this scenario, the MGF of y_a is given by

$$\mathbb{E}[e^{\theta y_a}] = \mathbb{E}[h_a^{\theta}] = \mathbb{E}[h_{a,LN}^{\theta}]\mathbb{E}[h_{a,RL}^{\theta}], \qquad \text{(A.1)}$$

where $h_{a,LN}$ is a lognormal RV, $h_{a,RL}$ a Rician RV, and both RVs are independent.
We know, from the lognormal case, that $y_{a,LN} = \log(h_{a,LN})$ is a Gaussian RV with mean $-\frac{\sigma_R^2}{2}$ and variance σ_R^2, and thus

$$\mathbb{E}[h_{a,LN}^{\theta}] = \mathbb{E}[e^{\theta y_{a,LN}}] = \exp\left(\frac{1}{2}\theta(\theta-1)\sigma_R^2\right). \qquad \text{(A.2)}$$

The PDF of $h_{a,RL}$ is

This article has been accepted for publication in a future issue of this journal, but has not been fully edited. Content may change prior to final publication. Citation information: DOI 10.1109/TWC.2017.2731947, IEEE Transactions on Wireless Communications

$$f_{h_{a,RL}}(x) = \frac{1+k^2}{\Omega}\exp\left(-k^2 - \frac{1+k^2}{\Omega}x\right)\mathrm{I}_0\left(2k\sqrt{\frac{1+k^2}{\Omega}x}\right) \tag{A.3}$$

$\mathbb{E}[h_{a,LN}^{\theta}]$ is given by

$$\mathbb{E}[h_{a,LN}^{\theta}] = \frac{(1+k^2)\exp(-k^2)}{\Omega}\times \int_0^{+\infty} x^{\theta}\exp\left(-\frac{1+k^2}{\Omega}x\right)\mathrm{I}_0\left(2k\sqrt{\frac{1+k^2}{\Omega}x}\right)dx \tag{A.4}$$

Using [29, Eq. (6.643.2)], we can write, for $\theta > -1$

$$\int_0^{+\infty} x^{\theta}\exp\left(-\frac{1+k^2}{\Omega}x\right)\mathrm{I}_0\left(2k\sqrt{\frac{1+k^2}{\Omega}x}\right)dx = \frac{\Gamma(\theta+1)}{k}\left(\frac{\Omega}{1+k^2}\right)^{\theta+1}\exp\left(\frac{k^2}{2}\right)M_{-\theta-\frac{1}{2},0}(k^2), \tag{A.5}$$

where $M_{\kappa,\mu}(\cdot)$ is the M-Whittaker function defined in [29, Sec. 9.220].
Using [46, Eq. (16.4.2a)], we have

$$M_{-\theta-\frac{1}{2},0}(k^2) = k\exp\left(-\frac{k^2}{2}\right){}_1F_1(1+\theta,1,k^2). \tag{A.6}$$

Using the property of the confluent hypergeometric F function given in [46, Eq. (16.1.6a)], we get

$$M_{-\theta-\frac{1}{2},0}(k^2) = k\exp\left(\frac{k^2}{2}\right){}_1F_1(-\theta,1,-k^2). \tag{A.7}$$

Replacing (A.7) in (A.5) and using this expression in (A.4), we get

$$\mathbb{E}[h_{a,LN}^{\theta}] = \left(\frac{\Omega}{1+k^2}\right)^{\theta}\Gamma(\theta+1)\ {}_1F_1(-\theta,1,-k^2). \tag{A.8}$$

Replacing (A.2) and (A.8) in (A.1), we get the desired result.

B. Málaga Turbulence

In the Málaga turbulence case, the MGF of y_a is

$$\mathbb{E}[h_a^{\theta}] = A\sum_{m=1}^{\beta} a_m \int_0^{+\infty} x^{\theta+\frac{\alpha+m}{2}-1}\mathrm{K}_{\alpha-m}\left(2\sqrt{\frac{\alpha\beta x}{g\beta+\Omega_0}}\right)dx \tag{A.9}$$

Using the change of variable $y = \sqrt{x}$, we can write

$$\int_0^{+\infty} x^{\theta+\frac{\alpha+m}{2}-1}\mathrm{K}_{\alpha-m}\left(2\sqrt{\frac{\alpha\beta x}{g\beta+\Omega_0}}\right)dx = 2\int_0^{+\infty} y^{2\theta+\alpha+m-1}\mathrm{K}_{\alpha-m}\left(2\sqrt{\frac{\alpha\beta}{g\beta+\Omega_0}}y\right)dy \tag{A.10}$$

Using [29, Eq. (5.561.16)], we get, for $m = 1,\ldots,\beta$

$$\int_0^{+\infty} x^{\theta+\frac{\alpha+m}{2}-1}\mathrm{K}_{\alpha-m}\left(2\sqrt{\frac{\alpha\beta x}{g\beta+\Omega_0}}\right)dx = \frac{1}{2}\left(\frac{g\beta+\Omega_0}{\alpha\beta}\right)^{\theta+\frac{\alpha+m}{2}}\Gamma(\theta+\alpha)\Gamma(\theta+m), \tag{A.11}$$

provided that $\theta > -\min(m,\alpha)$. Finally, we plug (A.11) in (A.9) to get the result, where θ need to satisfy $\theta > -\min(1,\alpha)$.

C. Double Generalized Gamma Turbulence

The MGF of y_a, in this setting, is given by

$$\mathbb{E}[e^{\theta y_a}] = \mathbb{E}[h_a^{\theta}] = \mathbb{E}[h_{a,1}^{\theta}]\mathbb{E}[h_{a,2}^{\theta}], \tag{A.12}$$

where here $h_{a,1}$ and $h_{a,2}$ are two independent Generalized Gamma RVs with parameters $(\alpha_1,\beta_1,\Omega_1)$ and $(\alpha_2,\beta_2,\Omega_2)$, respectively. We start by computing $\mathbb{E}[h_{a,1}^{\theta}]$

$$\mathbb{E}[h_{a,1}^{\theta}] = \frac{\alpha_1\beta_1^{\beta_1}}{\Omega_1^{\beta_1}\Gamma(\beta_1)}\int_0^{+\infty} x^{\theta+\alpha_1\beta_1-1}e^{-\frac{\beta_1}{\Omega_1}x^{\alpha_1}}dx \tag{A.13}$$

Using [29, Eq. (3.326.2)], we get, for $\theta > -\alpha_1\beta_1$

$$\mathbb{E}[h_{a,1}^{\theta}] = \left(\frac{\Omega_1}{\beta_1}\right)^{\frac{\theta}{\alpha_1}}\frac{\Gamma(\beta_1+\frac{\theta}{\alpha_1})}{\Gamma(\beta_1)}, \tag{A.14}$$

In a similar way, we have

$$\mathbb{E}[h_{a,2}^{\theta}] = \left(\frac{\Omega_2}{\beta_2}\right)^{\frac{\theta}{\alpha_2}}\frac{\Gamma(\beta_2+\frac{\theta}{\alpha_2})}{\Gamma(\beta_2)}, \tag{A.15}$$

with $\theta > -\alpha_2\beta_2$. Replacing (A.14) and (A.15) in (A.12), we get

$$\mathbb{E}[e^{\theta y_a}] = \left(\frac{\Omega_1}{\beta_1}\right)^{\frac{\theta}{\alpha_1}}\left(\frac{\Omega_2}{\beta_2}\right)^{\frac{\theta}{\alpha_2}}\frac{\Gamma\left(\beta_1+\frac{\theta}{\alpha_1}\right)\Gamma\left(\beta_2+\frac{\theta}{\alpha_2}\right)}{\Gamma(\beta_1)\Gamma(\beta_2)}, \tag{A.16}$$

with the condition $\theta > -\min(\alpha_1\beta_1,\alpha_2\beta_2)$.

APPENDIX B
SUB-OPTIMAL θ IN WEAK AND STRONG TURBULENCE REGIME

The MGF of the RV $y_a + y_p$ is given by

$$\mathcal{M}(\theta) = \mathbb{E}[e^{(y_a+y_p)\theta}] = \mathbb{E}[e^{\theta y_a}e^{\theta y_p}] = \mathbb{E}[e^{\theta y_a}]\mathbb{E}[e^{\theta y_p}], \tag{B.1}$$

where the last equality comes from the independence of y_a, and y_p. The CGF is then given by

$$\mu(\theta) = \log(\mathcal{M}_{y_a}(\theta)) + \log(\mathcal{M}_{y_p}(\theta)). \tag{B.2}$$

A. Lognormal Turbulence

For the lognormal turbulence, replacing $\mathcal{M}_{y_a}(\theta)$ by its expression and (25) in (B.2) , we get

$$\mu(\theta) = \log(\xi_x\xi_y) + \theta\log(A_0) - \frac{1}{2}\log((\xi_x^2+\theta)(\xi_y^2+\theta)) - \frac{2\theta}{w_{zeq}^2}\left[\frac{\mu_x^2\xi_x^2}{\xi_x^2+\theta} + \frac{\mu_y^2\xi_y^2}{\xi_y^2+\theta}\right] + \frac{1}{2}\theta(\theta-1)\sigma_R^2. \tag{B.3}$$

Replacing the derivative of (B.3) w.r.t θ in (27), we finally get the desired result in (41).

This article has been accepted for publication in a future issue of this journal, but has not been fully edited. Content may change prior to final publication. Citation information: DOI 10.1109/TWC.2017.2731947, IEEE Transactions on Wireless Communications

B. Rician-Lognormal Turbulence

In this case, the CGF is given by

$$\mu(\theta) = \log(\xi_x\xi_y) + \theta\log\left(\frac{A_0\Omega}{1+k^2}\right) - \frac{1}{2}\log((\xi_x^2+\theta)(\xi_y^2+\theta)) - \frac{2\theta}{w_{zeq}^2}\left[\frac{\mu_x^2\xi_x^2}{\xi_x^2+\theta} + \frac{\mu_y^2\xi_y^2}{\xi_y^2+\theta}\right] + \frac{1}{2}\theta(\theta-1)\sigma_R^2 + \log(\Gamma(1+\theta)) + \log({}_1F_1(-\theta,1,-k^2)). \tag{B.4}$$

Differentiating this equation w.r.t θ and replacing it in (27), we get (42).

C. Málaga Turbulence

The CGF in the Málaga turbulence is

$$\mu(\theta) = \log(\xi_x\xi_y) + \theta\log(A_0) - \frac{1}{2}\log((\xi_x^2+\theta)(\xi_y^2+\theta)) - \frac{2\theta}{w_{zeq}^2}\left[\frac{\mu_x^2\xi_x^2}{\xi_x^2+\theta} + \frac{\mu_y^2\xi_y^2}{\xi_y^2+\theta}\right] + \log\left(\frac{A}{2}\right)\log(\Gamma(\alpha+\theta)) + \log\left(\sum_{m=1}^{\beta} a_m\left(\frac{g\beta+\Omega_0}{\alpha\beta}\right)^{\frac{\alpha+m}{2}+\theta}\Gamma(\theta+m)\right). \tag{B.5}$$

Eq. (43) is then obtained by differentiating this equation w.r.t θ and setting it equal to ε, as per (27).

D. Double Generalized Gamma Turbulence

For the Double Generalized Gamma scenario, replacing $\mathcal{M}_{y_a}(\theta)$ by its expression and (25) in (B.2) , we get

$$\mu(\theta) = \log(\xi_x\xi_y) + \theta\log(A_0) - \frac{1}{2}\log((\xi_x^2+\theta)(\xi_y^2+\theta)) - \frac{2\theta}{w_{zeq}^2}\left[\frac{\mu_x^2\xi_x^2}{\xi_x^2+\theta} + \frac{\mu_y^2\xi_y^2}{\xi_y^2+\theta}\right] + \frac{\theta}{\alpha_1}\log\left(\frac{\Omega_1}{\beta_1}\right) + \frac{\theta}{\alpha_2}\times \log\left(\frac{\Omega_2}{\beta_2}\right) + \log\left(\Gamma\left(\beta_1+\frac{\theta}{\alpha_1}\right)\right) + \log\left(\Gamma\left(\beta_2+\frac{\theta}{\alpha_2}\right)\right) - \log\left(\Gamma(\beta_1)\Gamma(\beta_2)\right). \tag{B.6}$$

Taking the derivative of this equation w.r.t θ and replacing it in (27), we get (44).

Appendix C
Sampling from $f_{y_a}^*$ in lognormal turbulence regime

In weak turbulence, based on (6) and (23), the CDF is given by

$$F_{y_a}^*(t) = \frac{1}{\mathcal{M}_{y_a}(\theta)}\int_{-\infty}^{t}\frac{e^{\theta x}}{\sqrt{2\pi}\sigma_R}\exp\left(-\frac{(x+\frac{\sigma_R^2}{2})^2}{2\sigma_R^2}\right)dx = \frac{1}{\mathcal{M}_{y_a}(\theta)}\frac{1}{\sqrt{2\pi}\sigma_R}\int_{-\infty}^{t}\exp\left(-(\alpha x^2+2\beta x+\eta)\right)dx, \tag{C.1}$$

where $\alpha = \frac{1}{2\sigma_R^2}$, $\beta = \frac{1}{4} - \frac{\theta}{2}$, and $\eta = \frac{\sigma_R^2}{8}$. Using [29, Eq. (2.331)], we get

$$F_{y_a}^*(t) = \frac{1}{2}\left[\text{erf}\left(\frac{1-2\theta}{2\sqrt{2}}\sigma_R + \frac{x}{\sqrt{2}\sigma_R}\right)\right]_{-\infty}^{t} = \frac{1}{2}\left(1+\text{erf}\left(\frac{1-2\theta}{2\sqrt{2}}\sigma_R + \frac{t}{\sqrt{2}\sigma_R}\right)\right). \tag{C.2}$$

Finding u, such that $F_{y_a}^*(t) = u$, yields the inverse CDF given in (29).

Appendix D
Sampling from $f_{y_a}^*$ using [41]

In this appendix, we provide the algorithm for sampling from the biased PDFs based on [41]

Algorithm 1 Inverse transform sampling with Chebyshev approximation [41]

Input: PDF $f(x)$, finite interval $[a,b]$, number of samples N.

1: Construct an approximation $\tilde{f}$ of f on $[a,b]$

$$\tilde{f}(x) = \sum_{k=0}^{n}\alpha_k T_k\left(\frac{2(x-a)}{b-a} - 1\right),\ \alpha_k \in \mathbb{R},$$

2: Compute $\tilde{F}(x) = \int_x^a \tilde{f}(s)ds$ using Chebyshev polynomials integration properties.
3: Scale to a CDF if necessary, $\tilde{F}_X(x) = \tilde{F}(x)/\tilde{F}(b)$.
4: Generate random samples $\{U_i\}_{i=1}^N$ from the uniform distribution on $[0,1]$.
5: **for** $k = 1$ to N **do**
6: Solve $\tilde{F}_X(X_k) = U_k$ for X_k.
7: **end for**

Output: Samples $\{X_i\}_{i=1}^N$ drawn from the CDF $\tilde{F}_X$.

References

[1] C. B. Issaid, K.-H. Park, M.-S. Alouini, and R. Tempone, "Fast outage probability simulation for FSO links with a generalized pointing error model," in *Proceedings of IEEE Global Communications Conference (GC'16)*, Washington D.C., USA, Dec. 2016.

[2] S. Arnon, "Optimization of urban optical wireless communication systems," *IEEE Trans. Wireless. Commun.*, vol. 2, pp. 626–629, July 2003.

[3] A. Farid and S. Hranilovic, "Outage capacity optimization for free-space optical links with pointing errors," *IEEE/OSA J. Lightwave Technol.*, vol. 25, pp. 1702–1710, July 2007.

[4] W. Gappmair, S. Hranilovic, and E. Leitgeb, "OOK performance for terrestrial FSO links in turbulent atmosphere with pointing errors modeled by Hoyt distributions," *IEEE Commun. Letters*, vol. 15, pp. 875–877, Aug. 2011.

[5] F. Yang, J. Cheng, and T. A. Tsiftsis, "Free-space optical communication with nonzero boresight pointing errors," *IEEE Trans. Commun*, vol. 62, pp. 713–725, Feb 2014.

[6] H. Al-Quwaiee, H.-C. Yang, and M.-S. Alouini, "On the asymptotic ergodic capacity of FSO links with generalized pointing error model," in *Proceedings of IEEE*

International Conference on Communications (ICC'15), London, UK, June 2015.

[7] X. Zhu and J. M. Kahn, "Free-space optical communication through atmospheric turbulence channels," *IEEE Trans. Commun.*, vol. 50, pp. 1293–1300, Aug 2002.

[8] L. C. Andrews, R. L. Phillips, C. Y. Hopen, and M. A. Al-Habash, "Theory of optical scintillation," *J. Opt. Soc. Amer. A, Opt. Image Sci.*, vol. 16, pp. 1417–1429, June 1999.

[9] M. A. Al-Habash, L. C. Andrews, and R. L. Philips, "Mathematical model for the irradiance probability density function of a laser propagating through turbulent media," *Opt. Eng.*, vol. 40, pp. 1554–1562, Aug. 2001.

[10] I. S. Ansari, M.-S. Alouini, and J. Cheng, "Ergodic capacity analysis of free-space optical links with nonzero boresight pointing eorrors," *IEEE Trans. Wireless Commun*, vol. 14, pp. 4248–4264, Aug. 2015.

[11] I. S. Ansari, F. Yilmaz, and M.-S. Alouini, "Performance analysis of free-space optical links over Málaga ($\mathcal{M}$) turbulence channels with pointing errors," *IEEE Trans. Wireless Commun*, vol. 15, pp. 91–102, Jan. 2016.

[12] S. Kazemlou, S. Hranilovic, and S. Kumar, "All-optical multihop free-space optical communication systems," *Journal of Lightwave Technology*, vol. 29, no. 18, pp. 2663–2669, Sept 2011.

[13] M. Safari and M. Uysal, "Relay-assisted free-space optical communication," *IEEE Transactions on Wireless Communications*, vol. 7, no. 12, pp. 5441–5449, December 2008.

[14] N. A. M. Nor, Z. Ghassemlooy, J. Bohata, P. Saxena, M. Komanec, S. Zvanovec, M. Bhatnagar, and M. Khalighi, "Experimental investigation of all-optical relay-assisted 10 gbps fso link over the atmospheric turbulence channel," *Journal of Lightwave Technology*, vol. PP, no. 99, pp. 1–1, 2016.

[15] I. S. Ansari, F. Yilmaz, and M.-S. Alouini, "Impact of pointing errors on the performance of mixed RF/FSO dual-hop transmission systems," *IEEE Wireless Communications Letters*, vol. 2, pp. 351–354, June 2013.

[16] X. Tang, Z. Wang, Z. Xu, and Z. Ghassemlooy, "Multihop free-space optical communications over turbulence channels with pointing errors using heterodyne detection," *Journal of Lightwave Technology*, vol. 32, pp. 2597–2604, Aug 2014.

[17] E. Zedini and M.-S. Alouini, "Multihop relaying over im/dd fso systems with pointing errors," *Journal of Lightwave Technology*, vol. 33, pp. 5007–5015, Dec 2015.

[18] R. Srinivasan, *Importance Sampling - Applications in Communications and Detection*. Springer-Verlag, Berlin, 2002.

[19] K. B. Letaief and J. S. Sadowsky, "Computing bit-error probabilities for avalanche photodiode receivers by large deviations theory," *IEEE Trans. Inform. Theory*, vol. 38, pp. 1162–1169, Mar. 1992.

[20] P. Balaban, "Statistical evaluation of the error rate of the fiber-guide repeater using importance sampling," *Bell Syst. Tech. J.*, vol. 55, pp. 745–766, 1976.

[21] J.-C. Chen, D. Lu, J. S. Sadowsky, and K. Yao, "On importance sampling in digital communications-Part I: fundamentals," *IEEE J. Select. Areas Commun.*, vol. 11, pp. 289–299, 1993.

[22] P. J. Smith, M. Shafi, and H. Gao, "Quick simulation: a review of importance sampling techniques in communications systems," *IEEE J. on Sel. Areas in Comms.*, vol. 15, pp. 597–613, May 1997.

[23] A. Chaaban, J.-M. Morvan, and M.-S. Alouini, "Free-space optical communications: capacity bounds, aproximations, and a new sphere-packing perspective," *IEEE Trans. Commun*, vol. 64, pp. 1176–1191, Mar. 2016.

[24] S. Arnon, J. Barry, G. Karagiannidis, R. Schober, and M. Uysal, *Advanced optical wireless communications systems*. Cambridge University Press, 2013.

[25] A. Lapidoth, S. M. Moser, and M. A. Wigger, "On the capacity of free-space optical intensity channels," *IEEE Trans. Inf. Theory*, vol. 55, pp. 4449–4461, Oct. 2009.

[26] A. Goldsmith, *Wireless Communications*. Cambridge University Press, 2005.

[27] P. Beckmann and A. Spizzichino, *The Scattering of Electromagnetic Waves from Rough Surfaces*. Artech House, 1987.

[28] N. Perlot, *Characterization of Signal Fluctuations in Optical Communications With Intensity Modulation and Direct Detection Through the Turbulent Atmospheric Channel*. Berichte aus der Kommunikationstechnik, Shaker Verlag GmbH, 2005.

[29] I. S. Gradshteyn and I. M. Ryzhik, *Table of Integrals, Series, and Products*, seventh edition ed. Amsterdam: Elsevier/Academic Press, 2007.

[30] A. J. Navas, J. M. G. Balsells, J. F. Paris, and A. P. Notario, "A unifying statistical model for atmospheric optical scintillation," *Simulations of Physical and Engineering Processes*, pp. 181–206, Intech, 2011, ch. 8.

[31] E. Stacy, "A generalization of the Gamma distribution," *The Annals of Mathematical Statistics*, vol. 33, pp. 1187–1192, 1962.

[32] H. Al-Quwaiee, I. S. Ansari, and M.-S. Alouini, "On the performance of free-space optical communication systems over double generalized Gamma channel," *IEEE Journal on Selected Areas in Communications*, vol. 33, pp. 1829–1840, May 2015.

[33] N. B. Rached, F. Benkhelifa, M.-S. Alouini, and R. Tempone, "A fast simulation method for the log-normal sum distribution using a hazard rate twisting technique," in *Proceedings of IEEE International Conference on Communications (ICC'15)*, London, UK, June 2015.

[34] H. E. Daniels, "Saddlepoint approximations in statistic," *Ann. Math. Statis.*, vol. 5, pp. 631–650, 1954.

[35] R. Lugannani and S. Rice, "Saddlepoint approximation for the distribution of the sum of independent random variables," *Adv. in Appl. Probab*, vol. 12, pp. 475–490, 1980.

[36] J. A. Bucklew, *Large deviation techniques in decision, simulation, and estimation*. John Wiley, New York, 1990.

[37] M. K. Simon and M.-S. Alouini, *Digital Communication over Fading Channels*. Wiley, New York, 2005.

[38] L. U. Ancarani and G. Gasaneo, "Derivatives of any order of the confluent Hypergeometric function ${}_1F_1$(a,b,z) with respect to the parameter a or b," *Journal of Mathematical Physics*, vol. 49, pp. 3508–063 508, June 2008.

[39] D. P. Kroese, T. Taimre, and Z. I. Botev, *Handbook of Monte Carlo Methods*. New York: Wiley Series in Probability and Statistics, John Wiley & Sons, 2011.

[40] P. Glasserman, *Monte Carlo Methods in Financial Engineering*. Springer, New York, 2004.

[41] S. Olver and A. Townsend, "Fast inverse transform sampling in one and two dimensions," *ArXiv e-prints*, July 2013.

[42] ——. (2013) Matlab implementation of inverse transform sampling in 1D and 2D. [Online]. Available: https://github.com/dlfivefifty/InverseTransformSampling

[43] R. Boluda-Ruiz, A. Garcia-Zambrana, B. del Castillo-Vazquez, and C. del Castillo-Vazquez, "On the effect of correlated sways on generalized misalignment fading for terrestrial FSO links," *IEEE Photonics Journal*, vol. PP, no. 99, pp. 1–1, 2017.

[44] G. K. Karagiannidis, T. A. Tsiftsis, and R. K. Mallik, "Bounds for multihop relayed communications in nakagami-m fading," *IEEE Transactions on Communications*, vol. 54, pp. 18–22, Jan 2006.

[45] S. Bloom, E. Korevaar, J. Schuster, and H. Willebrand, "Understanding the performance of free-space optics," *J. Optical Networking*, vol. 2, pp. 178–200, June 2003.

[46] A. Cuyt, V. B. Petersen, B. Verdonk, H. Waadeland, and W. B. Jones, *Handbook of Continued Fractions for Special Functions*. Berlin: Springer-Verlag, 2008.

[47] A. Jeffrey, *Handbook of Mathematical Formulas and Integrals*, 3rd ed. Burlington: Academic Press, 2004.

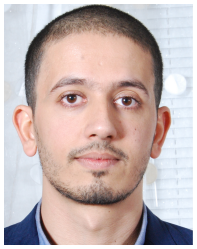

Chaouki Ben Issaid was born in Sfax, Tunisia. He received the Diplôme d'Ingénieur degree from l'École Polytechnique de Tunisie, La Marsa, Tunisia, in 2013. He also holds the Master degree in Applied Mathematics and Computational Science from King Abdullah University of Science and Technology (KAUST), Thuwal, Saudi Arabia. Currently, he is working toward the Ph.D degree in statistics at KAUST. His current research interests include efficient Monte Carlo simulations for the performance evaluation of wireless communication systems.

Ki-Hong Park (S'06, M'11) received his B.Sc. degree in Electrical, Electronic, and Radio Engineering from Korea University, Seoul, Korea, in 2005 and his M.S. and Ph.D. degrees in the School of Electrical Engineering from Korea University, Seoul, Korea, in 2011. Until 2014, he was a postdoctoral fellow is currently working for a research scientist in the Division of Physical Science and Engineering at King Abdullah University of Science and Technology (KAUST), Thuwal, Saudi Arabia. On-going research project is the design and analysis of optical wireless communication systems.

Mohamed-Slim Alouini (S'94, M'98, SM'03, F'09) was born in Tunis, Tunisia. He received the Ph.D. degree in Electrical Engineering from the California Institute of Technology (Caltech), Pasadena, CA, USA, in 1998. He served as a faculty member in the University of Minnesota, Minneapolis, MN, USA, then in the Texas A&M University at Qatar, Education City, Doha, Qatar before joining King Abdullah University of Science and Technology (KAUST), Thuwal, Makkah Province, Saudi Arabia as a Professor of Electrical Engineering in 2009. His current research interests include the modeling, design, and performance analysis of wireless communication systems.